

# UNCLASSIFIED

|   |
|---|
|   |
|   |
|   |
|   |
| AD NUMBER   |
| ADB265976   |
| NEW LIMITATION CHANGE   |
| TO<br>Approved for public release, distribution unlimited   |
| FROM<br>Distribution authorized to U.S. Gov't. agencies only; Proprietary Info.; Jul 2000. Other requests shall be referred to U.S. Army Medical Research and Materiel Command, 504 Scott St., Fort Detrick, MD 21702-5012. |
| AUTHORITY   |
| USAMRMC ltr, 26 Aug 2002  |

THIS PAGE IS UNCLASSIFIED

AD\_\_\_\_\_

Award Number: DAMD17-98-1-8228

TITLE: Analysis of Ligand Binding ErbB Receptor Tyrosine Kinases

PRINCIPAL INVESTIGATOR: Kathryn Ferguson, Ph.D.

Mark A. Lemmon, Ph.D.

CONTRACTING ORGANIZATION: University of Pennsylvania  
Philadelphia, Pennsylvania 19104-3246

REPORT DATE: July 2000

TYPE OF REPORT: Annual Summary

PREPARED FOR: U.S. Army Medical Research and Materiel Command  
Fort Detrick, Maryland 21702-5012

DISTRIBUTION STATEMENT: Distribution authorized to U.S. Government agencies only (proprietary information, Jul 00). Other requests for this document shall be referred to U.S. Army Medical Research and Materiel Command, 504 Scott Street, Fort Detrick, Maryland 21702-5012.

The views, opinions and/or findings contained in this report are those of the author(s) and should not be construed as an official Department of the Army position, policy or decision unless so designated by other documentation.

20010509 022

**REPORT DOCUMENTATION PAGE**Form Approved  
OMB No. 074-0188

Public reporting burden for this collection of information is estimated to average 1 hour per response, including the time for reviewing instructions, searching existing data sources, gathering and maintaining the data needed, and completing and reviewing this collection of information. Send comments regarding this burden estimate or any other aspect of this collection of information, including suggestions for reducing this burden to Washington Headquarters Services, Directorate for Information Operations and Reports, 1215 Jefferson Davis Highway, Suite 1204, Arlington, VA 22202-4302, and to the Office of Management and Budget, Paperwork Reduction Project (0704-0188), Washington, DC 20503

|   |   |  |  |                               |
|---|---|--|--|-------------------------------|
| <b>1. AGENCY USE ONLY (Leave blank)</b>   |   | <b>2. REPORT DATE</b><br>July 2000                                 | <b>3. REPORT TYPE AND DATES COVERED</b><br>Annual Summary (1 Jul 99 - 30 Jun 00) |                               |
| <b>4. TITLE AND SUBTITLE</b><br>Analysis of Ligand Binding ErbB Receptor Tyrosine Kinases   |   |  | <b>5. FUNDING NUMBERS</b><br>DAMD17-98-1-8228                                    |                               |
| <b>6. AUTHOR(S)</b><br>Kathryn Ferguson, Ph.D.<br>Mark A. Lemmon, Ph.D.   |   |  |  |                               |
| <b>7. PERFORMING ORGANIZATION NAME(S) AND ADDRESS(ES)</b><br>University of Pennsylvania<br>Philadelphia, Pennsylvania 19104-3246<br><br><b>E-MAIL:</b><br>ferguso2@mail.med.upenn.edu   |   |  | <b>8. PERFORMING ORGANIZATION<br/>REPORT NUMBER</b>                              |                               |
| <b>9. SPONSORING / MONITORING AGENCY NAME(S) AND ADDRESS(ES)</b><br><br>U.S. Army Medical Research and Materiel Command<br>Fort Detrick, Maryland 21702-5012  |   |  | <b>10. SPONSORING / MONITORING<br/>AGENCY REPORT NUMBER</b>                      |                               |
| <b>11. SUPPLEMENTARY NOTES</b>  |   |  |  |                               |
| <b>12a. DISTRIBUTION / AVAILABILITY STATEMENT</b><br>Distribution authorized to U.S. Government agencies only (proprietary information, Jul 00).<br>Other requests for this document shall be referred to U.S. Army Medical Research and Materiel<br>Command, 504 Scott Street, Fort Detrick, Maryland 21702-5012.  |   |  |  | <b>12b. DISTRIBUTION CODE</b> |
| <b>13. ABSTRACT (Maximum 200 Words)</b><br><br>Growth factor-receptor tyrosine kinases (RTK's) play a central role in the coordination of cell growth, differentiation and other activities in multicellular organism. Molecular lesions in and/or aberrant expression of RTK's can lead to cancer. There is a particularly strong correlation between the erbB2 (neu/HER-2) receptor and breast cancer. The cell-surface location of the erbB2 receptor makes it an obvious target for novel therapies. The purpose of this research is to gain insight into the structure of the extracellular domain of this receptor and its mode of activation in order to aid in the development of new antagonists. ErbB2 is one of a family of 4 RTK's which also includes the epidermal growth factor receptor (EGFR). The first step in the stimulation of a response by a growth factor is dimerization of the receptor upon binding of the cognate ligand. We have crystals of the EGF induced homodimer of the soluble extracellular domain of EGFR. Determination of this structure is in progress, and several derivatives have been identified. This structure will provide insight into the specific molecular events that drive erbB receptor dimerization. A key question is whether the dimerization is mediated only by receptor-receptor contacts, or whether the ligand is bivalent in nature, simultaneously contacting both receptor molecules in the dimer. |   |  |  |                               |
| <b>14. SUBJECT TERMS</b><br>ErbB Receptor: Growth Factor: Ligand Binding: X-ray Crystallography: Protein Structure: Breast<br>Cancer  |   |  | <b>15. NUMBER OF PAGES</b><br>24   |                               |
|   |   |  | <b>16. PRICE CODE</b>  |                               |
| <b>17. SECURITY CLASSIFICATION<br/>OF REPORT</b><br>Unclassified  | <b>18. SECURITY CLASSIFICATION<br/>OF THIS PAGE</b><br>Unclassified | <b>19. SECURITY CLASSIFICATION<br/>OF ABSTRACT</b><br>Unclassified | <b>20. LIMITATION OF ABSTRACT</b><br>Unlimited                                   |                               |

## FOREWORD

Opinions, interpretations, conclusions and recommendations are those of the author and are not necessarily endorsed by the U.S. Army.

AMS Where copyrighted material is quoted, permission has been obtained to use such material.

Where material from documents designated for limited distribution is quoted, permission has been obtained to use the material.

AMS Citations of commercial organizations and trade names in this report do not constitute an official Department of Army endorsement or approval of the products or services of these organizations.

N/A In conducting research using animals, the investigator(s) adhered to the "Guide for the Care and Use of Laboratory Animals," prepared by the Committee on Care and use of Laboratory Animals of the Institute of Laboratory Resources, national Research Council (NIH Publication No. 86-23, Revised 1985).

N/A For the protection of human subjects, the investigator(s) adhered to policies of applicable Federal Law 45 CFR 46.

N/A In conducting research utilizing recombinant DNA technology, the investigator(s) adhered to current guidelines promulgated by the National Institutes of Health.

N/A In the conduct of research utilizing recombinant DNA, the investigator(s) adhered to the NIH Guidelines for Research Involving Recombinant DNA Molecules.

N/A In the conduct of research involving hazardous organisms, the investigator(s) adhered to the CDC-NIH Guide for Biosafety in Microbiological and Biomedical Laboratories.

AM Livingston  
PI - Signature

7/28/00

Date

## Table of Contents

|                              |          |
|------------------------------|----------|
| Front Cover                  |          |
| Standard Form 298            | page 2   |
| Foreword                     | page 3   |
| Table of Contents            | page 4   |
| Introduction                 | page 5   |
| Body of Report               | page 5   |
| Key Research Accomplishments | page 9   |
| Reportable Outcomes          | page 9   |
| Conclusions                  | pages 9  |
| References                   | page 10  |
| Appendices                   | pages 11 |

## Introduction

Growth factor-receptor tyrosine kinases (RTK's) play a central role in the coordination of cell growth, differentiation and other activities in multicellular organism<sup>1</sup>. Molecular lesions in and/or aberrant expression of RTK's can lead to cancer. There is a particularly strong correlation between the erbB2 (neu/HER-2) receptor and breast cancer<sup>2-5</sup>. The cell-surface location of the erbB2 receptor makes it an obvious target for novel therapies. The purpose of this research is to gain insight into the structure of the extracellular domain of this receptor and its mode of activation in order to aid in the development of new antagonists. ErbB2 is one of a family of 4 RTK's which also includes the epidermal growth factor receptor (EGFR). The first step in the stimulation of a response by a growth factor is dimerization of the receptor upon binding of the cognate ligand<sup>6-7</sup>. We have crystals of the EGF induced homodimer of the soluble extracellular domain of EGFR that diffract to better than 2.8 Å. Determination of this structure is in progress. This structure will provide insight into the specific molecular events that drive erbB receptor dimerization. A key question is whether the dimerization is mediated only by receptor-receptor contacts, or whether the ligand is bivalent in nature, simultaneously contacting both receptor molecules in the dimer.

## Body of Annual Report

Most of the effort of this funding period has been directed toward accomplishing Task 5; solving the X-ray crystal structure of the s-erbB1/EGF complex. The problem of crystal non-isomorphism has been solved and we can proceed with determining the phase information needed to solve the structure. The native data that we now have is sufficient to solve the structure once phases have been obtained. We hope to be able to obtain higher resolution data in the future.

### **Task 1 Obtain purified receptor extracellular domains (months 1 - 18)**

As described in detail in our 1999 annual report, the full length extracellular domains of erbB1, 2, 3 and 4 (s-erbBs) can be expressed in insect cells using recombinant baculoviruses and purified to homogeneity. This procedure is now routine and performed by a number of members of the laboratory to produce protein for different experiments.

### **Task 2. Obtain purified ligands (months 1 - 18)**

We purchase all ligands from commercial sources and use them without further purification. High quality s-erbB1/EGF crystals can be grown using EGF purchased from Interger, which is relatively inexpensive. We have available *E. coli* or yeast systems for several ligands which we will use if necessary. Work will proceed on this task as required.

### **Task 3. Characterize binding of ligands to isolated domains 1 and 3 (months 6 - 12)**

In the interest of diverting full effort towards solving the structure of the full length s-erbB1 ectodomain in complex with EGF (Task 5), this task has been postponed until a later stage in the funding period.

### **Task 4. Obtain diffraction quality crystals of s-erbB1/EGF complex (months 7 - 18)**

As described in detail in the 1999 annual report, diffraction quality crystals of the s-erbB1/EGF complex have been obtained. Good crystals diffract to better than 3.5 Å on a MAR image plate detector using double mirror-monochromated/focused Cu K<sub>α</sub> X-rays from a Siemens generator. The crystals are of

space group C2, with  $a = 118 \text{ \AA}$ ,  $b = 103 \text{ \AA}$ ,  $c = 100 \text{ \AA}$ ,  $\beta = 119^\circ$  and one half dimer per asymmetric unit. There is variability in the diffraction quality of the crystals and many have to be tested to find a strong single, crystal. Seeding has been successfully applied and improves reproducibility and quality of the crystals. This project represents a key component in several beam time applications at both the National Synchrotron Light Source at Brookhaven National Laboratories and the Cornell High Energy Synchrotron Source (CHESS).

#### **Task 5. Solve the X-ray crystal structure (months 18 - 30)**

##### **(i) Collect high resolution native data (months 18 - 24)**

A complete native data set to  $2.8 \text{ \AA}$  has been collected on an unstabilized frozen crystal at the National Synchrotron Light Source (NSLS) beam line X25 operating at  $1.0 \text{ \AA}$  with a Brandeis 4-module CCD-Based detector (B4) Data were processed using DENZO and SCALEPACK<sup>8</sup>. A summary of the data collection statistics was given in the last report. While the data extend to  $2.8 \text{ \AA}$  the quality of the high resolution data is poor. Current focus has been toward obtaining data from a stabilized crystals as detailed below. Once phases have been obtained and the structure solved further attempts will be made to obtain the highest resolution data possible.

##### **(ii) Search for heavy atom derivative (months 18 - 30) and**

##### **(iii) Collect heavy atom derivative data (months 18 - 30)**

The first stage in initiating a heavy atom derivative search is to ensure that a crystal soaked in stabilizer without any heavy atom added is isomorphous with native data. As detailed in 1999 annual report, problems were encounter at this step. The stabilized crystals were non-isomorphous with the crystal frozen after only brief exposure to the cryoprotectant (as used to collect the data at NSLS X25). This problem has been resolved. We have recently been able to collect a complete data set at NSLS beam line X12B on a crystal stabilized for 24 hours. Data were collected at  $1.0 \text{ \AA}$ , with a Area Detector Systems Corporation Quantum 4 CCD detector (Q4), and were processed with MOSFLM<sup>9</sup> and CCP4<sup>10,11</sup>. Statistics for the data set are presented in Table 1.

| Resolution Shells |      | Unique Reflections | Completeness | $R_{\text{sym}}$ | $I/\sigma$ |
|-------------------|------|--------------------|--------------|------------------|------------|
| 50.00             | 6.26 | 2293               | 95.5         | 0.038            | 15.2       |
| 6.26              | 5.11 | 1926               | 97.0         | 0.038            | 15.6       |
| 5.11              | 4.43 | 2290               | 97.8         | 0.039            | 14.8       |
| 4.43              | 3.96 | 2601               | 98.0         | 0.044            | 14.1       |
| 3.96              | 3.61 | 2879               | 98.5         | 0.064            | 9.3        |
| 3.61              | 3.35 | 3157               | 98.7         | 0.089            | 7.8        |
| 3.35              | 3.13 | 3361               | 98.9         | 0.142            | 5.2        |
| 3.13              | 2.95 | 3602               | 99.1         | 0.254            | 2.9        |
| 2.95              | 2.80 | 3814               | 99.2         | 0.411            | 1.8        |
| All reflections   |      | 25923              | 98.2         | 0.057            | 9.5        |

**Table 1.** Data collection statistics for native data from a stabilized crystal collected at NSLS X12B.

The quality of the data from this crystal is improved compared to the data collected at beam line X25, although the overall intensity is a little weaker. The photon flux at beam line X12B is substantially lower than at beam line X25 ( $\approx 30$  fold). It is anticipated that this stabilized crystal will yield higher resolution data at either NSLS beam line X25 or CHESS beam line F1. We have time at CHESS F1 in September of this year. The photon flux at CHESS F1 is at least as good as NSLS X25.

Three methods are being explored to determine the phase information required to solve the structure. For discussion these methods will be considered separately, although information from each approach may be combined in producing the final phases to calculate an interpretable electron density map.

(a) The use of multiple isomorphous replacement (MIR) is being explored. In this method the positions of heavy atoms in multiple different derivatives of the crystal are used to solve the phase problem. The conventional method for obtaining heavy atom derivative is to soak the crystal in solutions containing a variety of different heavy metal ions. These ions can interact with accessible functional groups in the protein crystal such as those on methionines and histidines.

A number of potential heavy atom derivatives are currently being analyzed. This analysis is greatly aided by the new native data that we collected at X12B. Table 2 shows details some of the data that we are analyzing and the merging R-factor to the X12B data ( $R_{iso}$ ).

| Heavy Atom                       | Soak Condition | X-ray Source         | Resolution Limit | Completeness (multiplicity) | I/ $\sigma$ (mean) | $R_{sym}$ | $R_{iso}$ |
|----------------------------------|----------------|----------------------|------------------|-----------------------------|--------------------|-----------|-----------|
| PIP (Pt)                         | 1 mM 18 h      | Home                 | 3.8 Å            | 95 % (3.5)                  | 15.6               | 0.09      | 16.6 %    |
| PIP (Pt)                         | 1 mM 18 h      | X12B $\lambda=0.9$ Å | 3.5 Å            | 55 % (2.0)                  | 12.2               | 0.06      | 16.7 %    |
| K <sub>2</sub> PtCl <sub>4</sub> | 1 mM 15 h      | Home                 | 3.8 Å            | 52 % (2.8)                  | 10.5               | 0.09      | 18.8 %    |
| KAuI <sub>4</sub>                | 5 mM 24 h      | Home                 | 3.2 Å            | 91 % (2.8)                  | 17.6               | 0.06      | 12.6 %    |
| UO <sub>2</sub> SO <sub>4</sub>  | 1 mM 18 h      | Home                 | 3.8 Å            | 61 % (2.2)                  | 12.7               | 0.09      | 13.8 %    |

**Table 2.** Data collected for EGF:s-erbB1 crystals soaked with different heavy-atom compounds. PIP, di- $\mu$ -iodobis(ethylenediamine)diplatinum dinitrate; UO<sub>2</sub>SO<sub>4</sub>, uranyl sulfate

We are currently trying to identify heavy atom sites in these derivatives by analyzing isomorphous and anomalous difference Patterson maps, using the programs MLPHARE<sup>12</sup> and SOLVE<sup>13</sup>. We have two candidate heavy atom sites for the PIP derivative that are currently being refined and checked. Preliminary analysis indicates that this would be a rather poor derivative and would not contribute greatly to the final phases. However at this stage identifying and characterizing a derivative is a major advance.

(b) Recent developments open the possibility that we may be able to solve the structure using the multiwavelength anomalous diffraction (MAD) phasing method<sup>14,15</sup>. In this method data from a single crystal containing several anomalous scatterers (e.g. selenium atoms) are collected at several different wavelengths. We will generate crystals of a selenomethionine derivative of s-erbB1 in complex with wild type EGF (EGF has no methionines). There are 10 methionines in the 621 amino acids of mature s-erbB1, and alignment with the IGF1-R structure (see below) indicates that at least half of these will be in well-ordered regions. If high-efficiency substitution with selenomethionine can be achieved at these positions, there is a significant chance that the EGF:s-erbB1 complex can be solved using MAD phasing.

The selenomethionine (Se-Met) is incorporated biosynthetically by expressing the protein in cells that have Se-Met as the only source of methionine. We have performed this many times to produce Se-Met proteins in *E. coli*. The application of this method to protein expressed in insect cells is relatively new<sup>16-18</sup>.



Bellizzi *et al* have modified and optimized the method for expression of secreted proteins and have solved the structure of an insect cell expressed secreted protein using the MAD method<sup>18,19</sup>. We have expressed a selenomethionine analogue of s-erbB1 (Figure 1). Sf21 cells are grown in standard serum free medium and infected with recombinant virus as usual. Thirty six hours after infection with virus the cells are collected by centrifugation, and transferred to a medium containing no methionine. Cells are incubated in this medium for 4 hours to allow methionine to be cleared from the cells. Following this clearing period cells transferred to methionine minus medium containing 50 mg/L selenomethionine. After a further 3 days, the conditioned media is harvested and the Se-Met erbB1 purified as for the wild type protein. Pilot analysis indicated that the expression level is not compromised by the use of Se-Met (Figure 1). Large scale production of this derivative is currently in progress. We hope to be able to have crystals ready and tested by September when we have beam time at CHESS F1. At that time we hope to be able to collect a single wavelength experiment. This will allow us to find the Se sites in the crystal. If crystals look promising we will put in a separate synchrotron beam time request for time to perform a full MAD experiment.

(c) The final method that may be useful in gaining phasing information is molecular replacement (MR). The 2.6 Å resolution x-ray crystal structure of the first three extracellular domains (ECD) of the insulin-like growth factor type 1 receptor (IGF-1R) has been solved<sup>20</sup> and the coordinates have now become available. The first three subdomains of the IGF1-R ECD are closely related to the first three (of four) subdomains in s-erbB1. Subdomains 1 and 3 of s-erbB1, which share 31% identity, align well with subdomains L1 and L2 of the IGF1-R ECD. Subdomains L1 and L2 of IGF1-R share 22% identity, and the C<sub>α</sub> positions of their respective β-helix structures superimpose with a root-mean-squared deviation of 1.6 Å. The sequences of IGF1-R L1 and L2 align better with D1 and D3 of s-erbB1 than they do with one another (Figure 2), suggesting that s-erbB1 subdomains D1 and D3 will have similar β-helix structures. Molecular replacement has been attempted using L1, L2, and L1 plus L2 as search models, using AmoRe<sup>21</sup> and the Patterson correlation technique in XPLOR<sup>22</sup>. Initial search models were generated by trimming all non-conserved side-chains to the β-carbon. Thus far no clear solution has been obtained. Since appropriately trimmed L1 and L2 search models together correspond to only around 30% of the scattering power of our EGF:s-erbB1 crystal asymmetric unit (assuming 59% solvent content), it is not surprising that a solution has not been obtained easily. A direction currently under investigation is to use a theoretical model proposed for s-erbB1 on the basis of the x-ray crystal structure of IGF-1R<sup>23</sup> as a molecular replacement search model.

### Key Research Accomplishments

- Native data from a stabilized EGF/s-erbB1 crystals to 2.8 Å resolution has been collected
- Conditions to generate selenomethionine s-erbB1 have been established
- A platinum EGF/s-erbB1 derivative has been identified.

### Reportable Outcomes

#### Manuscripts:

Ferguson, K.M., Darling, P.J., Macatee, T.L., Mohan, M. and Lemmon, M.A. (2000) Extracellular Domains Drive Homo- but not Hetero-Dimerization of ErbB Receptors. *EMBO J.* in press.

#### Abstracts:

Ferguson, K.M., Macatee, T.L., and Lemmon, M.A. (2000) Extracellular Domains are sufficient for ligand-induced homo- but not hetero-dimerization of erbB receptors. Era of Hope Meeting for the Department of Defense Breast Cancer Research Program.

Ferguson, K.M., and Lemmon, M.A. (2000) Structural Analysis of ligand binding by the epidermal growth factor receptor family of tyrosine kinases. Era of Hope Meeting for the Department of Defense Breast Cancer Research Program.

#### Grant Support:

|           |                         |                |
|-----------|-------------------------|----------------|
| NIH Grant | R21-CA87182-01 (Lemmon) | 7/1/00-6/30/03 |
| NIH/NCI   |                         | \$ 75,000      |

Based upon the results obtained by the PI during the period of this award, Mark A. Lemmon, the PI's mentor, has applied for and been granted a NIH Insight Award to complete the structure of the erbB1/EGF complex and initiate attempts to crystallize erbB2. This grant will provide salary for a technical assistant and supplies. In addition it will provide salary for the PI in subsequent years to allow continuation on this research beyond the end of this DOD BCRP award.

### Conclusions

Major advances have been made towards gaining the phasing information required to solve the crystal structure of the EGF induced s-erbB1 homodimer. We have identified one heavy atom derivative, and can generate selenomethionine protein that may allow the use of the MAD phasing method.

Knowledge of the structure of the EGF activated erbB1 dimer will be extremely valuable in understanding the mechanism of activation of the erbB family of receptors. The ultimate goal of this study is to gain a structural view of the ectodomain of erbB2 in a ligand induced heterodimer with erbB1. In turn this should allow design of novel strategies for therapeutic intervention in breast cancer.

## References

1. Ullrich, A. & Schlessinger, J. (1990) Signal transduction by receptors with tyrosine kinase activity. *Cell* **61**, 203-212.
2. Hynes, N.E. & Stern, D.F. (1994) The biology of *erbB-2/neu/HER-2* and its role in cancer. *Biochim. Biophys. Acta* **1198**, 165-184.
3. Slamon, D.J., Goldolphin, W., Jones, L.A., Holt, J.A., Wong, S.G., Keith, D.E., Levin, W.J., Stuart, S.G., Udove, J., Ullrich, A. & Press, M.F. (1989) Studies of the *HER-2/neu* proto-oncogene in human breast and ovarian cancer. *Science* **244**, 707-712.
4. Dougall, W.C., Qian, X., Peterson, N.C., Miller, M.J., Samanta, A. & Greene, M.I. (1994) The neu oncogene: Signal transduction pathways, transformation mechanisms and evolving therapies. *Oncogene* **9**, 2109-2123.
5. Bacus, S.S., Zelnick, C.R., Plowman, G. & Yarden, Y. (1994) Expression of the *erbB-2* family of growth factor receptors and their ligands in breast cancers. Implication for tumor biology and clinical behavior. *Am. J. Clin. Pathol.* **102**, S13-24.
6. Lemmon, M.A. & Schlessinger, J. (1994) Regulation of signals transduction and signal diversity by receptor oligomerization. *Trends Bioc. Sci.* **19**, 459-463.
7. Lemmon, M.A. & Schlessinger, J. (1997) Transmembrane signaling by receptor oligomerization. In *Methods in Molecular Biology*, Vol 84: *Transmembrane Signaling Protocols* (Bar-Sagi, D., ed.) Humana Press Inc., Totowana, NJ, pp 31-53.
8. Otwinowski, Z. & Minor, W. (1997) Processing of x-ray diffraction data collection in oscillation mode. *Methods Enzymol.* **276** 307-326
9. Leslie, A.G.W. (1992) Joint CCP4 & ESF-EAMCB Newsletter on Protein Crystallography, No. 26.
10. Collaborative Computational Project, Number 4 (1994) "The CCP4 Suite: Programs for Protein Crystallography". *Acta Cryst.* **D50**, 760-763
11. P.R.Evans (1993) "Data reduction", Proceedings of CCP4 Study Weekend on Data Collection & Processing, pp 114-122
12. Otwinowski, Z. (1991). ML-PHARE CCP4 Proc. 80-88 (Daresbury Laboratory, Warrington, UK).
13. Terwilliger, T.C., and Berendzen, J. (1996) Correlated phasing of multiple isomorphous replacement data. *Acta Cryst.* **D52**, 749-757.
14. Hendrickson, W.A., Smith, J.L., Phizackerley, R.P., and Merritt, E.A. (1988) Crystallographic structure analysis of lamprey hemoglobin from anomalous dispersion of synchrotron radiation. *Proteins: Struct., Funct., & Genet.* **4**, 77-88.
15. Hendrickson, W.A., Pahler, A., Smith, J.L., Satow, Y., Merritt, E.A., and Phizackerley, R.P. (1989) Crystal structure of core streptavidin determined from multiwavelength anomalous diffraction of synchrotron radiation. *Proc. Natl. Acad. Sci. U.S.A.* **86**, 2190-2194.
16. Chen, W., and Bahl, O.P. (1991) Recombinant carbohydrate and selenomethionyl variants of human choriogonadotropin. *J. Biol. Chem.* **266**, 8192-8197.
17. Chen, W., and Bahl, O.P. (1991) Selenomethionyl analog of recombinant human choriogonadotropin. *J. Biol. Chem.* **266**, 9355-9358.
18. Bellizzi, J.J., Widom, J., Kemp, C.W., Clardy J (1999) Producing selenomethionine-labeled proteins with a baculovirus expression vector system. *Structure Fold Des.* **7**, R263-7.
19. Bellizzi, J.J., Widom, J., Kemp, C., Lu, J.Y., Das, A.K., Hofmann, S.L., Clardy J. (2000) The crystal structure of palmitoyl protein thioesterase 1 and the molecular basis of infantile neuronal ceroid lipofuscinosis. *Proc Natl Acad Sci (U S A)* **97**, 4573-4578.
20. Garrett, T.P.J, McKern, N.M., Lou, M., Frenkel, M.J., Bentley, J.D., Lovrecz, G.O., Elleman, T.C., Cosgrove, L.J. & Ward, C.W. (1998) Crystal structure of the first three domains of the type-1 insulin-like growth factor receptor. *Nature* **394**, 395-399.
21. Navaza, J. (1994) AMoRe: An automated package for molecular replacement. *Acta Cryst. A* **50**, 157-163.
22. Brünger, A.T. (1992a). XPLOR Version 3.1. A System for X-Ray Crystallography and NMR (New Haven, Connecticut: Yale University Press).
23. Jorissen, R.N., Epa, V.C., Treutlein, H.R., Garrett, T.P., Ward, C.W., Burgess, A.W. (2000) Characterization of a comparative model of the extracellular domain of the epidermal growth factor receptor. *Protein Sci* **9**, 310-324.

## Appendices

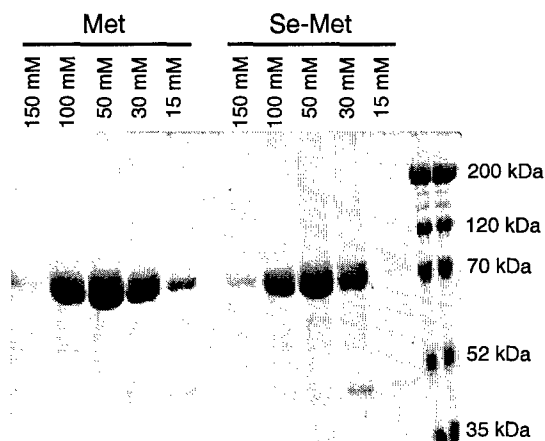


**Figure 1** Coomassie stained SDS-PAGE of Met s-erbB1 and Se-Met s-erbB1. Duplicate cultures of Sf21 cells were infected with recombinant s-erbB1, and treated as described in text. For samples on the left, 50 mg/L methionine was added in the final incubation period, whereas for samples on the right, 50 mg/L for selenomethionine was used. Fractions eluting from a Ni-NTA column with increasing concentrations of imidazole are shown for each case. As is evident the expression levels are only slightly reduced when using the Se-Met.

```

IGF1R L1  EICGP...GIDIRN.....DYQQLKRLNCTVIEGYLHILLISKA.....EDYRS
EGFR D1   KVCQ....GTSNKLTLGLTFEDHFLSLQRMFNCEVVLGNLEITYVQRN.....YD
EGFR D3   KVCN....GIGIGEFKDSLST..NATNIKHFRNCTSSISGDLHLPLVAFRGDSFTHTPPLDPQE
IGF1R L2  KVCEEEKTKTID.....SVTSAQMLQGCTIFKGNLLINIRGN.....NIASELE

IGF1R L1  YRFPKLT.VITEYLLFRVAGLESGLDFPNLTVIRGWKLFY.NYALVTFEMTNLKDIGL...
EGFR D1   LSFLKTIQEVAGYVLIALNT.VERI..PLENLQIIRGNMYEYNSYALAVLSNYDANKTGLKEL
EGFR D3   LDILKTVKEITGFLLIQAWPENRTDLHAFENLEIIRGRTKQHGQFSLAVVSL.NITSLGL...
IGF1R L2  NFMGLIE.VVTGYVKIRHSHALVSL.SFLKNLRLILGEEQLEGNYSEFYVLDNQNLQQLWDW..

IGF1R L1  ..YNLRNITIRGAIRIEKNADLCYLSTVDWSLILD...AVSNNTIV..GNKPPKECGD
EGFR D1   PMRNLQEIILHGAVRFSNNPALCNVESIQWRDIVS...SDFLSNMSMDFQNLHGSCQK
EGFR D3   ..RSLKEISDGDVVISGNKNLCYANTINWKKLFGT..SGQKTKII..SNRGENSCKA
IGF1R L2  DHRNL.TIKASKMYFAFNPKLCVSEIYRMEEVVTGKGRQSKGDIINTRNNGERASCES

```

**Figure 2** Alignment of the ligand-binding subdomains of EGF receptor (D1 and D3) with the equivalent subdomains in the IGF1 receptor ECD (L1 and L2). Sequence identities in the alignments are:  $L1_{IGF1-R}/L2_{IGF1-R}$ , 22%;  $D1_{erbB1}/D3_{erbB1}$ , 31%;  $L1_{IGF1-R}/D1_{erbB1}$ , 25%;  $L1_{IGF1-R}/D3_{erbB1}$ , 29%;  $L2_{IGF1-R}/D1_{erbB1}$ , 26%;  $L2_{IGF1-R}/D3_{erbB1}$ , 25%.

## Extracellular domains drive homo- but not hetero-dimerization of erbB receptors

Kathryn M. Ferguson, Paul J. Darling,  
Mohita Mohan, Timothy L. Macatee and  
Mark A. Lemmon<sup>1</sup>

Department of Biochemistry & Biophysics and Johnson Research  
Foundation, University of Pennsylvania School of Medicine,  
Philadelphia, PA 19104-6059, USA

<sup>1</sup>Corresponding author

Many different growth factor ligands, including epidermal growth factor (EGF) and the neuregulins (NRGs), regulate members of the erbB/HER family of receptor tyrosine kinases. These growth factors induce erbB receptor oligomerization, and their biological specificity is thought to be defined by the combination of homo- and hetero-oligomers that they stabilize upon binding. One model proposed for ligand-induced erbB receptor hetero-oligomerization involves simple heterodimerization; another suggests that higher order hetero-oligomers are 'nucleated' by ligand-induced homodimers. To distinguish between these possibilities, we compared the abilities of EGF and NRG1- $\beta$ 1 to induce homo- and hetero-oligomerization of purified erbB receptor extracellular domains. EGF and NRG1- $\beta$ 1 induced efficient homo-oligomerization of the erbB1 and erbB4 extracellular domains, respectively. In contrast, ligand-induced erbB receptor extracellular domain hetero-oligomers did not form (except for s-erbB2-s-erbB4 hetero-oligomers). Our findings argue that erbB receptor extracellular domains do not recapitulate most heteromeric interactions of the erbB receptors, yet reproduce their ligand-induced homo-oligomerization properties very well. This suggests that mechanisms for homo- and hetero-oligomerization of erbB receptors are different, and contradicts the simple heterodimerization hypothesis prevailing in the literature.

**Keywords:** dimerization/growth factor/scattering/  
signaling/tyrosine kinase

### Introduction

The epidermal growth factor (EGF) receptor is the prototype of the erbB family of receptor tyrosine kinases (RTKs) that also includes erbB2 (HER-2 or Neu), erbB3 (HER-3) and erbB4 (HER-4) (Carraway and Cantley, 1994; Alroy and Yarden, 1997; Riese and Stern, 1998). Each erbB receptor contains an extracellular ligand-binding domain of 600-630 amino acids, a single transmembrane  $\alpha$ -helix, plus an intracellular domain of ~600 amino acids that includes the tyrosine kinase and regulatory sequences (Schlessinger and Ullrich, 1992). It was established more than a decade ago for the EGF receptor (erbB1) that growth factor-induced receptor

oligomerization is critical for transmembrane signaling (Schechter *et al.*, 1979; Schlessinger, 1979; Yarden and Schlessinger, 1987a,b). It is now generally accepted that the cytoplasmic tyrosine kinases of two (or more) RTKs in a growth factor-induced dimer (or larger oligomer) mutually activate one another through transphosphorylation (Honegger *et al.*, 1990; Lemmon and Schlessinger, 1994; Heldin, 1995; Hubbard *et al.*, 1998). Several downstream signaling molecules are then recruited to the phosphorylated receptor, specified by its complement of regulatory tyrosine phosphorylation sites (Songyang *et al.*, 1993; Schlessinger, 1994).

Many cells co-express multiple members of the erbB receptor family, which can form both homo- and hetero-oligomers upon stimulation with growth factor ligands (Heldin, 1995). Oligomers containing almost every possible pairwise combination of erbB receptors have now been reported (reviewed by Carraway and Cantley, 1994; Alroy and Yarden, 1997; Riese and Stern, 1998). The earliest evidence for hetero-oligomerization of erbB receptors came from the finding that erbB2 can be activated by EGF, despite the fact that it does not bind directly to this ligand. EGF is only able to activate erbB2 when erbB1 is also present in the same cell, suggesting 'transmodulation' of erbB2 as a result of its EGF-induced hetero-oligomerization with erbB1 (King *et al.*, 1988; Stern and Kamps, 1988; Wada *et al.*, 1990; Goldman *et al.*, 1990; Spivak-Kroizman *et al.*, 1992).

There are >10 distinct ligands that activate erbB receptors. Three of these have been classified as 'EGF agonists' (Riese and Stern, 1998), since they bind directly to only erbB1 [EGF, transforming growth factor- $\alpha$  (TGF- $\alpha$ ) and amphiregulin]. Four (or more) of the ligands are specific for erbB3 and/or erbB4 (the neuregulins; NRGs), while a further three have been classified as 'bispecific' and bind directly to both erbB1 and erbB4 [betacellulin, epiregulin and possibly heparin-binding EGF-like factor (HB-EGF)] (Riese and Stern, 1998; Harari *et al.*, 1999; J.T.Jones *et al.*, 1999, and references therein). The EGF agonists activate erbB1 when it is expressed alone, but also transmodulate erbB2, erbB3 and erbB4 in an erbB1-dependent manner. Similarly, the NRGs activate erbB4 directly, but can also transactivate erbB1 or erbB2 when erbB4 or erbB3 are also present (Riese *et al.*, 1995). Finally, the bispecific ligands appear to activate erbB1 and erbB4 when either is expressed alone, and to transmodulate erbB2 and erbB3 via these receptors (reviewed by Alroy and Yarden, 1997; Riese and Stern, 1998). ErbB2, which is of particular medical interest as a target of breast cancer therapies (Sliwkowski *et al.*, 1999), has no known ligand and can only be activated *in trans* by ligands in these three classes. In fact, erbB2 is considered to be a preferred hetero-oligomerization partner for all of the

other erbB receptors (Karunagaran *et al.*, 1996; Graus-Porta *et al.*, 1997).

Several possible mechanisms for erbB receptor transmodulation have been considered. In the simplest and most often discussed, transmodulation is proposed to result from ligand-induced receptor heterodimerization (Alroy and Yarden, 1997; Burden and Yarden, 1997; Riese and Stern, 1998). According to this mechanism, a ligand stimulates two receptors to come together. If the two receptors are identical, this is homodimerization; if not, it is heterodimerization. Either way, the two receptors in the dimer become activated by transphosphorylation, and transmembrane signaling is achieved. Several studies argue that erbB receptor extracellular domains are sufficient for their hetero-oligomerization (Qian *et al.*, 1994), and combinatorial receptor (homo- or hetero-) dimerization could be driven by simultaneous binding of bivalent erbB ligands to the extracellular domains of two receptor molecules (Lemmon *et al.*, 1997; Tzahar *et al.*, 1997). Different bivalent ligands could stabilize distinct receptor homo- and/or heterodimers depending on the combination of binding sites that they contain.

An alternative view is that growth factors such as EGF induce only homodimerization of the erbB receptors to which they bind directly. The resulting receptor homodimers may then activate *in trans* the erbB receptors to which the ligand does not bind, through quite different mechanisms. For example, transmodulation of erbB2 by EGF could simply involve phosphorylation of erbB2 as a substrate for the activated EGF receptor. Another possibility (Huang *et al.*, 1998) is that EGF-induced erbB1 homodimers could provide an interface at which dimerization of erbB2 is promoted. ErbB2 could thus become activated by 'proxy' in the context of an (erbB1)<sub>2</sub>(erbB2)<sub>2</sub> heterotetramer. A model of this sort could explain the surprising observation that a kinase-negative form of erbB1 can transmodulate erbB2 upon EGF binding (Wright *et al.*, 1995).

In order to determine whether erbB receptor homo- and hetero-oligomerization occur through similar mechanisms, we have studied the effects of ligand binding on the

assembly of isolated erbB receptor extracellular domains. We reported previously that the isolated erbB1 extracellular domain (s-erbB1) homodimerizes quantitatively upon binding to EGF or TGF- $\alpha$  (Lemmon *et al.*, 1997). Here, we show that NRG1- $\beta$ 1 can also induce homo-oligomerization of the erbB4 extracellular domain. In contrast, ligand-induced hetero-oligomerization appears to be the exception rather than the rule for erbB receptor extracellular domains. While NRG1- $\beta$ 1 can induce the formation of hetero-oligomers that contain the erbB2 and erbB4 extracellular domains, no evidence could be obtained for EGF-induced formation of any extracellular domain hetero-oligomer. These findings indicate that erbB receptors form homo- and hetero-oligomers through quite different mechanisms, and that transmodulation of erbB receptors is most probably nucleated by a ligand-induced erbB1 or erbB4 homodimer.

## Results

### High-affinity ligand binding by recombinant s-erbB proteins

To investigate the ligand binding and dimerization properties of soluble erbB receptor extracellular domains (s-erbBs), we first established methods for their production in milligram quantities by secretion from baculovirus-infected Sf9 cells (Figure 1). Using surface plasmon resonance (BIAcore), we next measured binding of each purified s-erbB protein to both EGF and NRG1- $\beta$ 1 that were immobilized on BIAcore CM-5 sensor chips. The s-erbB proteins were passed across these surfaces at a variety of concentrations, and the maximum response observed was plotted against s-erbB concentration to generate the binding curves shown in Figure 2A. As anticipated, s-erbB1 bound strongly to the EGF-derivatized sensor surface ( $K_D = 118$  nM), but not to surfaces carrying NRG1- $\beta$ 1 or to surfaces with no ligand. Both s-erbB3 and s-erbB4 bound strongly to the NRG1- $\beta$ 1 surface ( $K_D$  values of 249 and 179 nM, respectively; see Table I), but not to the EGF-derivatized surface. In contrast, s-erbB2 did not bind to any of the surfaces tested (Figure 2A). We repeated these experiments using 1:1 mixtures of different s-erbB proteins (e.g. s-erbB2 plus s-erbB3 or s-erbB4) to determine whether free s-erbB proteins might hetero-oligomerize, leading to significant alterations in their apparent ligand-binding affinities. In these studies, mixing s-erbB proteins had no detectable influence on their ligand-binding properties (not shown), arguing that s-erbB hetero-oligomers (if they form) do not bind the immobilized ligands with a significantly higher affinity than single s-erbB species.

### s-erbB1 and s-erbB4 homo-oligomerize upon ligand binding, while s-erbB3 does not

To analyze ligand-induced dimerization of s-erbB proteins, we employed multi-angle laser light scattering (MALLS) and sedimentation equilibrium analytical ultracentrifugation, both of which give information on molecular mass changes that is independent of molecular shape (Cantor and Schimmel, 1980).

**Multi-angle laser light-scattering studies.** MALLS allows the weight-averaged molecular mass ( $\bar{M}_w$ ) of proteins in solution to be measured rapidly over a wide

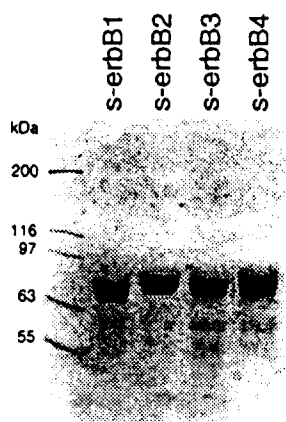


Fig. 1. SDS-PAGE (7.5%) of the purified s-erbB proteins used for analysis of ligand-induced homo- and hetero-oligomerization. Purified protein (15  $\mu$ l) was loaded at a concentration of 1 mg/ml, and the gel was stained with Coomassie blue. Molecular mass standards were loaded in the left-most lane, and are marked.

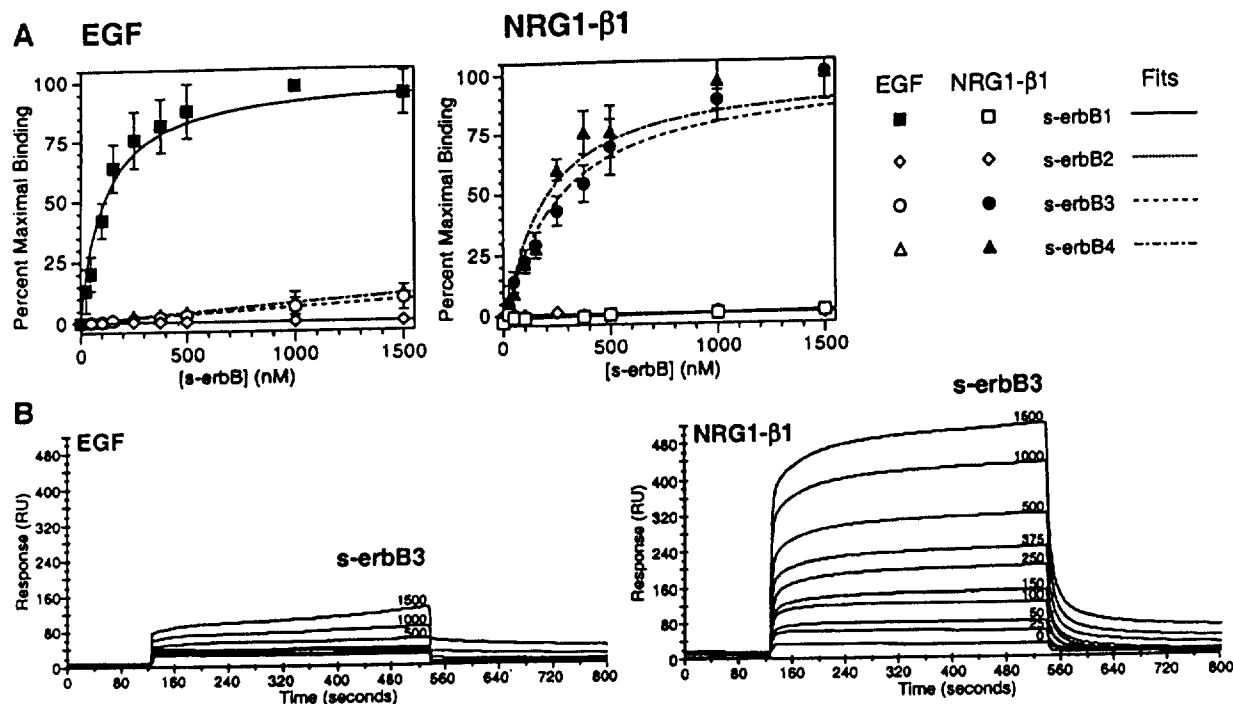


Fig. 2. (A) Data for binding of s-erbB1, s-erbB2, s-erbB3 and s-erbB4 to EGF (left) and NRG1-β1 (right), immobilized on a BIAcore sensor chip. Best fits to the data, assuming a simple association model, are shown. Errors are standard deviations from the mean of at least four independent determinations at each point.  $K_D$  values represented by the best fits are listed in Table I. (B) Representative raw BIAcore data for s-erbB3 flowed in parallel over a biosensor chip derivatized with EGF (left) and NRG1-β1 (right) at a series of different concentrations (marked on each curve in nM).

Table I. Ligand binding by s-erbB proteins

| Ligand | $K_D$ (nM)   |         |              |              |
|--------|--------------|---------|--------------|--------------|
|        | s-erbB1      | s-erbB2 | s-erbB3      | s-erbB4      |
| EGF    | $118 \pm 41$ | none    | $>10^4$      | $>10^4$      |
| NRG-β1 | $>10^4$      | none    | $249 \pm 80$ | $179 \pm 10$ |

$K_D$  values measured using BIAcore for binding of s-erbB proteins to immobilized EGF and NRG1-β1. Means of at least four independent determinations are quoted alongside their standard deviations.

range of protein concentrations (see Materials and methods). MALLS measurements gave an  $\bar{M}_w$  value of  $77 \pm 8$  kDa for purified s-erbB1 alone. When EGF is titrated effectively into an s-erbB1 solution (with fixed s-erbB1 concentration),  $\bar{M}_w$  increases in a linear fashion until one molar equivalent of EGF has been added to s-erbB1 (Figure 3A). At this point,  $\bar{M}_w$  is 2.2-fold higher than that measured for s-erbB1 alone, suggesting EGF-induced formation of a dimeric complex containing two EGF molecules plus two molecules of s-erbB1, as we have observed with other methods (Lemmon *et al.*, 1997). No further increase in  $\bar{M}_w$  is seen when EGF is added in excess, arguing that higher order oligomers of s-erbB1 do not form. The curve through the data in Figure 3A represents the results expected if EGF binds to monomeric s-erbB1 with a  $K_D = 118$  nM (Table I), and the resulting 1:1 (EGF:s-erbB1) complex dimerizes completely. The  $K_D$  for this dimerization event (which is complete at 4  $\mu$ M s-erbB1) appears to be  $<0.1$   $\mu$ M, based on additional

MALLS studies at low concentration and gel filtration experiments (not shown).

Similar MALLS studies of s-erbB4 gave a  $\bar{M}_w$  of  $82 \pm 6$  kDa that increased by a factor of  $>2$  as NRG1-β1 was added (Figure 3B). In this case, the maximum  $\bar{M}_w$  value was not reached until more than two equivalents of NRG1-β1 had been added. Furthermore, the final  $\bar{M}_w$  value ( $\sim 235$  kDa) was higher than expected for a dimeric s-erbB4-NRG1-β1 complex. These data therefore suggest that NRG1-β1 is able to induce formation of s-erbB4 oligomers that are larger than dimers. Without more detailed analysis at significantly higher protein concentrations and at larger excesses of ligand, we cannot determine the maximum oligomeric state. However, an increase of nearly 3-fold in  $\bar{M}_w$  (at an NRG1-β1:s-erbB4 ratio of 3:1) is equally consistent with the formation of s-erbB4 trimers and with the formation of a mixture that contains 50% of the s-erbB4 as dimers plus 50% as tetramers.

We also used MALLS to analyze the ability of NRG1-β1 to induce s-erbB3 oligomerization. As shown by a single data point in Figure 3B (and confirmed in centrifugation studies described below), addition of a 2-fold excess of NRG1-β1 did not increase the  $\bar{M}_w$  measured for s-erbB3 above that measured for s-erbB3 alone ( $90 \pm 4$  kDa). This finding is consistent with a previous report (Horan *et al.*, 1995), and does not reflect a lack of NRG1-β1 binding by s-erbB3 (see Figure 2B and Table I). Addition of neither EGF (Figure 3A) nor NRG1-β1 (not shown) altered the value measured for s-erbB2 ( $78 \pm 10$  kDa), as expected since neither ligand binds to this protein (Figure 2A).

**Analytical ultracentrifugation.** Sedimentation equilibrium experiments gave the same results for ligand-induced

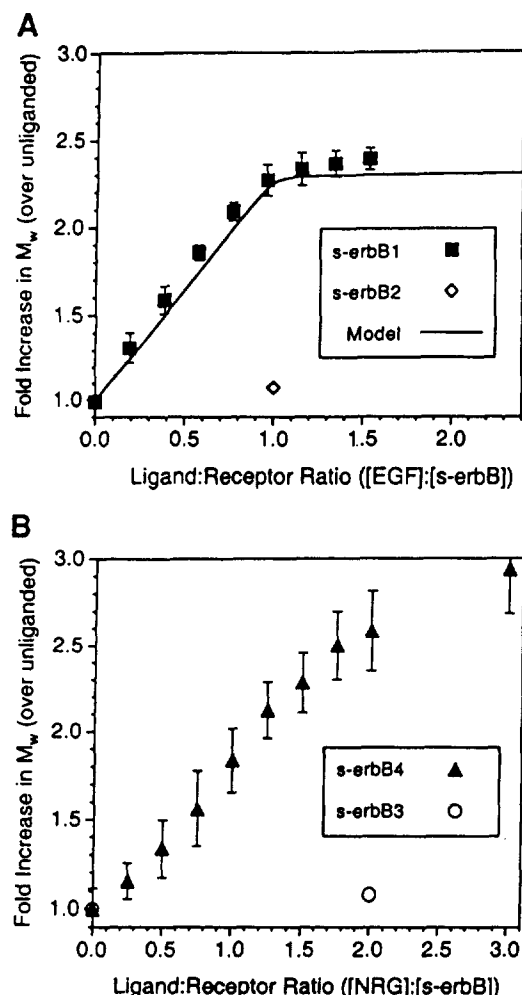


**Fig. 3.** MALLS studies of EGF-induced homodimerization of s-erbB1- (A) and NRG1- $\beta$ 1-induced homo-oligomerization of s-erbB4 (B). The weight-averaged molecular mass ( $M_w$ ) of s-erbB1:EGF mixtures (relative to for s-erbB1 alone), as determined by MALLS (see Materials and methods), is plotted against the EGF:s-erbB1 ratio in the mixture. Quantitative EGF-induced s-erbB1 homodimerization is shown (filled squares). The solid line represents the expected results for a model in which EGF binds s-erbB1 with a  $K_D$  of 118 nM, and the resulting 1:1 complex dimerizes with a  $K_D$  of 100 nM (see text). The single open diamond in (A) shows one point for a similar experiment with s-erbB2, demonstrating that s-erbB2 does not dimerize when EGF is added (see also Figure 4B). In (B), the same experiment is shown for NRG1- $\beta$ 1 binding to s-erbB4 (filled triangles), which it causes to oligomerize. Also in (B), a single point (open circle) shows the failure of NRG1- $\beta$ 1 to induce s-erbB3 homo-oligomerization. Error bars correspond to the standard deviations for the mean of three or more experiments. The concentration of s-erbB protein was 4  $\mu$ M in each experiment.

s-erbB protein homo-oligomerization. Figure 4 shows typical data from sedimentation equilibrium experiments (at 6000 r.p.m.) in which 5  $\mu$ M samples of each s-erbB protein were centrifuged both with (filled symbols) and without (open symbols) a 2-fold molar excess of the most relevant growth factor ligand. Data obtained with the ligand-free s-erbB proteins can be fit, using a model that assumes a single non-ideal species, to give molecular mass estimates of  $81 \pm 1$  kDa (s-erbB1),  $80 \pm 3$  kDa (s-erbB2),  $82 \pm 7$  kDa (s-erbB3) and  $81 \pm 3$  kDa (s-erbB4). The residuals for these fits, plotted above the data in Figure 4,

are both small and random, indicating good fits. When EGF is added to s-erbB1 (Figure 4A), or NRG1- $\beta$ 1 is added to s-erbB4 (Figure 4D), the radial distribution plots suggest a substantial increase in molecular mass (with material accumulating at higher radii). Since the molecular masses of EGF and NRG1- $\beta$ 1 are only 6 and 8 kDa, respectively (Lemmon *et al.*, 1997; data not shown), and those of s-erbB1 and s-erbB4 are  $\sim 80$  kDa, this effect can only be explained by homo-oligomerization of the s-erbB proteins upon addition of the relevant growth factor. The data for s-erbB:ligand mixtures can be fit using a model that assumes two ideal species: the ligand-receptor complex and excess ligand. Using this model, the masses of s-erbB1-EGF and s-erbB4-NRG1- $\beta$ 1 complexes are estimated as  $159 \pm 10$  kDa and  $146 \pm 18$  kDa, respectively (residuals for these fits are shown in Figure 4A and D), consistent with the ligand-induced oligomerization of these extracellular domains seen by MALLS. In other sedimentation experiments (not shown), TGF- $\alpha$  and HB-EGF were also found to induce formation of s-erbB1 homo-oligomers (assumed dimers). As with MALLS, sedimentation equilibrium studies of s-erbB4:NRG1- $\beta$ 1 mixtures at higher s-erbB4 concentrations and larger ligand excesses (not shown) suggested that NRG1- $\beta$ 1 induces formation of s-erbB4 oligomers larger than dimers. However, we have not yet been able to determine whether these are trimers or mixtures of different oligomers.

In contrast to the findings for s-erbB1 and s-erbB4, no indication of ligand-induced oligomerization was seen when EGF was added to s-erbB2 (Figure 4B), or when NRG1- $\beta$ 1 was added to either s-erbB3 (Figure 4C) or s-erbB2 (see below). The data for the s-erbB2:EGF mixture were best fit as a combination of free EGF and free s-erbB2 ( $82 \pm 12$  kDa), and those for the s-erbB3:NRG1- $\beta$ 1 mixture fit best as free NRG1- $\beta$ 1 (8 kDa) plus a 1:1 s-erbB3-NRG1- $\beta$ 1 complex of  $83 \pm 17$  kDa.

#### **ErbB1 and erbB2 extracellular domains do not heterodimerize upon EGF binding**

Having confirmed that EGF induces s-erbB1 homodimerization, and that NRG1- $\beta$ 1 induces s-erbB4 homo-oligomerization, we next investigated the ability of erbB ligands to induce heterodimerization of erbB receptor extracellular domains. As described in the Introduction, the most well-studied example of erbB receptor transmodulation involves erbB1 and erbB2. Since EGF induces complete homodimerization of s-erbB1, we expected from the simple heterodimerization model for erbB receptor transmodulation that EGF should also induce the formation of s-erbB1-s-erbB2 heterodimers.

Contrary to these expectations, heterodimer formation could not be observed in MALLS studies when EGF was added to a 1:1 mixture of s-erbB1 and s-erbB2. Instead, EGF induced homodimerization of s-erbB1 in the mixture, while s-erbB2 remained monomeric. As shown in Figure 5A, titration of EGF into a solution containing 4  $\mu$ M (crossed-squares) or 8  $\mu$ M (filled squares) s-erbB1 alone caused complete dimerization.  $M_w$  reached a maximum value ( $\sim 2$ -fold) after addition of EGF to  $\sim 4$  and 8  $\mu$ M, respectively, as expected for the formation of a 2:2 EGF:s-erbB1 dimer. If EGF-induced heterodimeriza-



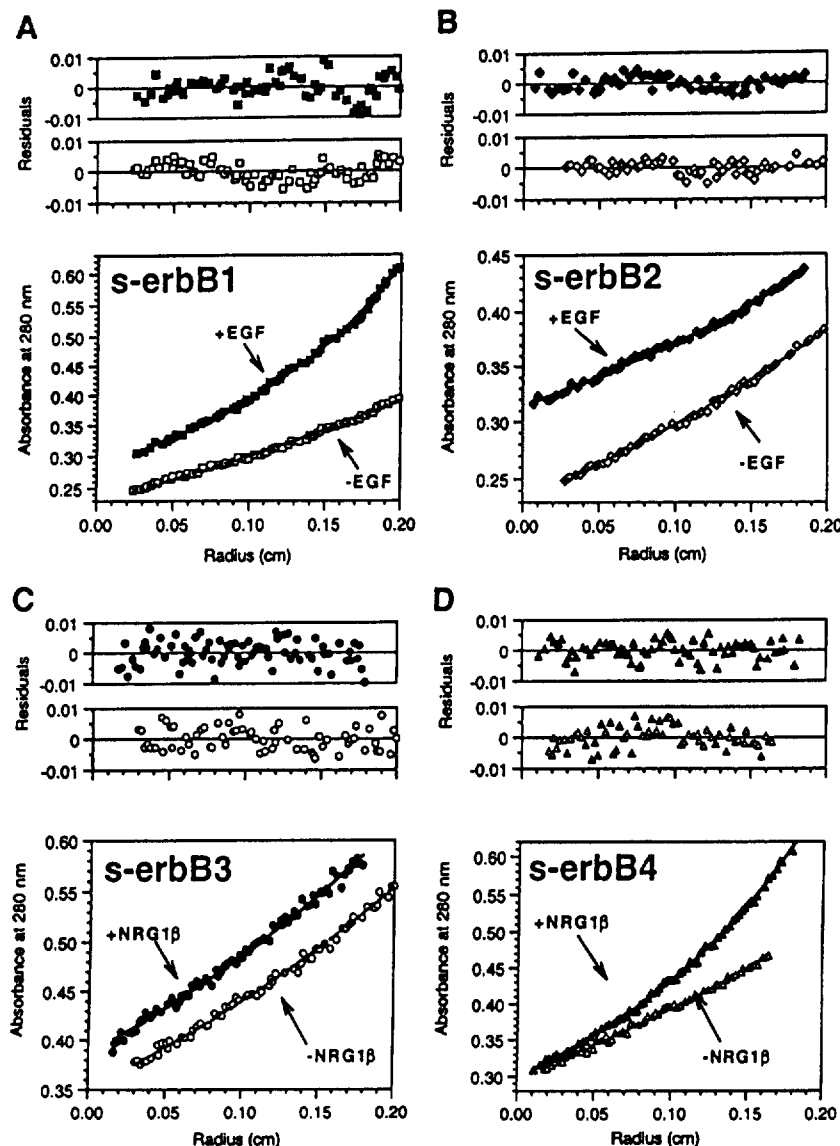


**Fig. 4.** Representative sedimentation equilibrium analytical ultracentrifugation data for analysis of s-erbB homo-oligomerization induced by EGF or NRG1- $\beta$ 1. In each case, open symbols represent s-erbB protein without added ligand, which is fit as a single non-ideal species. Filled symbols represent samples to which a 2-fold molar excess of the noted ligand has been added. As discussed in the text, fits to these data are with two ideal species (complex plus excess free ligand)—fixing the mass of the ligand and floating the mass of the complex. Purified s-erbB protein was used at 5  $\mu$ M for each sample. All experiments shown were performed at 6000 r.p.m. Repeats at 9000 and 12 000 r.p.m. gave the same results. Residuals for the fits described above are shown, and are seen to be both small and random, indicative of a good fit. EGF induced homo-oligomerization of s-erbB1 only, while NRG1- $\beta$ 1 induced homo-oligomerization of s-erbB4 only.

tion of s-erbB1 with s-erbB2 were similarly strong, MALLS data for a 1:1 s-erbB1:s-erbB2 mixture (8  $\mu$ M total receptor) should resemble that seen for 8  $\mu$ M s-erbB1 alone. However, EGF addition to such a 1:1 mixture (diamonds in Figure 5A) induced a maximum  $\bar{M}_w$  increase of only 1.6-fold, and this maximum was reached at 4  $\mu$ M, not 8  $\mu$ M, total EGF. Homodimerization of just s-erbB1 (at 4  $\mu$ M) in this mixture would be maximal at 4  $\mu$ M EGF according to the data in Figure 3A. Furthermore, a 1.6-fold increase in  $\bar{M}_w$  is exactly what is expected if s-erbB1 homodimerizes (yielding 174 kDa s-erbB1 dimers at 2  $\mu$ M) while s-erbB2 remains monomeric (80 kDa s-erbB2 monomers at 4  $\mu$ M). Therefore, EGF does not induce heterodimerization of s-erbB1 with s-erbB2—or at least the  $K_D$  for this heterodimerization event is sufficiently

weak to be undetectable under these conditions (where s-erbB1 homodimerization is complete).

Sedimentation equilibrium experiments also argue strongly against EGF-induced s-erbB1-s-erbB2 heterodimerization. For a set of experiments performed at 6000 r.p.m., the natural logarithm of absorbance at 290 nm (proportional to protein concentration) is plotted in Figure 5B against  $(r^2 - r_0^2)/2$ , where  $r$  is the radial position in the sample, and  $r_0$  the radial position of the meniscus. For an ideal single species, this plot is linear and the gradient of the line  $[\bar{M}\omega^2(1 - \bar{V}_2\rho/RT)]$  is proportional to the molecular mass ( $M$ ) of the ideal species (Cantor and Schimmel, 1980). The data for s-erbB1 or s-erbB2 alone fit well to a straight line with a gradient that suggests a molecular mass of ~80 kDa in each case. When two molar

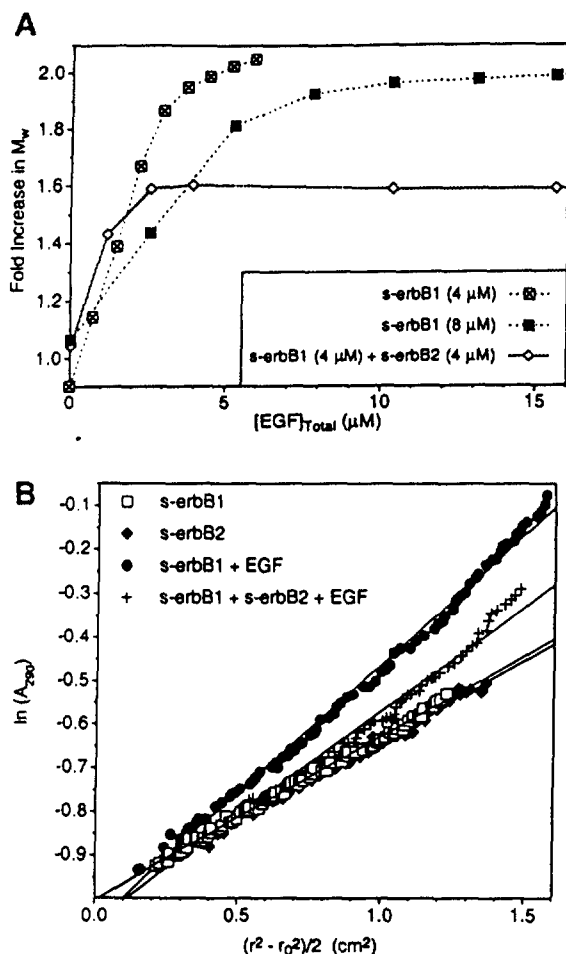


Fig. 5. (A) A MALLS experiment demonstrating that, while EGF induces complete homo-dimerization of s-erbB1 at 4  $\mu$ M (crossed squares) or 8  $\mu$ M (filled squares), it does not induce the formation of heterodimers between s-erbB2 and s-erbB1 (open diamonds). The experiment was performed as described for Figure 3. With 4  $\mu$ M s-erbB1, complete dimerization is seen after addition of 4  $\mu$ M EGF (note that the horizontal axis here is EGF concentration, and not ligand:receptor ratio). With 8  $\mu$ M s-erbB1, addition of 8  $\mu$ M EGF is required for complete dimerization. When the 1:1 s-erbB1:s-erbB2 mixture is studied, with a total s-erbB protein concentration of 8  $\mu$ M, only 4  $\mu$ M EGF is required for maximal dimerization, and the maximum fold increase in  $M_w$  is consistent only with a mixture of s-erbB1 homodimers and s-erbB2 monomers. Lines are drawn to guide the eye, and do not represent fits to the data. (B) Plots of the natural logarithm of absorbance at 290 nm (monitoring protein concentration) against a function of the radius squared ( $r^2 - r_0^2$ )/2 (see text for explanation) for sedimentation equilibrium analytical ultracentrifugation data obtained at 6000 r.p.m. with s-erbB1 and s-erbB2. For an ideal single species, this representation of the data should appear as a straight line with a gradient proportional to the molecular mass (see text). When analyzed alone, both s-erbB1 (open squares) and s-erbB2 (filled diamonds) yield good straight lines, with gradients proportional to their monomeric molecular masses (see also fits in Figure 4). Each sample contained a total s-erbB concentration of 10  $\mu$ M. The increase in gradient for the s-erbB1/s-erbB2/EGF mixture (crosses) is consistent with the formation of s-erbB1 homodimers only.

equivalents of EGF were added to s-erbB1, the gradient of the best straight line (filled squares) was increased substantially over that for s-erbB1 alone, because of EGF-induced s-erbB1 homodimerization. When the same

excess of EGF was added to a 1:1 s-erbB1:s-erbB2 mixture (two EGFs added per s-erbB molecule), the data fit less well to a straight line (indicating multiple species), and the gradient of the best line was increased only slightly over that for s-erbB1 or s-erbB2 alone. Similar experiments at substantially higher receptor concentrations also failed to provide evidence for erbB1-erbB2 hetero-oligomerization. Thus, as seen with MALLS, analytical ultracentrifugation studies suggest that EGF induces homodimerization of s-erbB1 in a s-erbB1:s-erbB2 mixture, while s-erbB2 remains monomeric.

These biophysical studies show that the isolated extracellular domains of erbB1 and erbB2 do not associate with one another in a heterodimer (or any other oligomer) upon EGF addition, whereas s-erbB1 homodimerizes efficiently upon EGF binding (Figures 3, 4 and 5) and EGF-dependent co-immunoprecipitation of intact erbB1 and erbB2 has been reported by many groups. In studies not shown, we attempted to detect s-erbB1-s-erbB2 interactions using chemical cross-linking and co-immunoprecipitation approaches, and obtained only negative results (although s-erbB1 homodimers could be seen readily by chemical cross-linking). We therefore suggest that, while the extracellular domain is sufficient for EGF-induced homodimerization of erbB1, extracellular domains are not capable of driving receptor hetero-oligomerization. Before concluding this, however, an important caveat must be considered. Since erbB2 has no known ligand, we cannot validate the functional integrity of Sf9 cell-derived s-erbB2 by virtue of its ligand binding, as was possible with s-erbB1, s-erbB3 and s-erbB4 (Figure 2). However, we believe that s-erbB2 is functional, since it appears to form NRG1-induced hetero-oligomers with s-erbB4 (see below).

**ErbB1 and erbB4 extracellular domains do not hetero-oligomerize upon EGF or NRG1- $\beta$ 1 binding**  
Evidence for hetero-oligomerization (or transmodulation) of erbB1 and erbB4 upon treatment of cells with either EGF or NRG has been reported by several groups (Riese *et al.*, 1995, 1996; Cohen *et al.*, 1996; Zhang *et al.*, 1996; F.E.Jones *et al.*, 1999). We therefore used analytical ultracentrifugation to investigate whether EGF and NRG1- $\beta$ 1 induce s-erbB1-s-erbB4 heterodimerization. Since we know that s-erbB1 and s-erbB4 are both competent to homo-oligomerize upon binding of EGF and NRG1- $\beta$ 1, respectively, we can be confident that these proteins are functionally active.

A series of sedimentation equilibrium experiments was performed with 1:1 mixtures of s-erbB1 and s-erbB4, with the same total receptor concentration (8  $\mu$ M) in each case (Figure 6). When no ligand was added, the gradient of the straight line through the data gives an average monomeric molecular mass of ~80 kDa. Addition of EGF to a concentration twice that of total receptor (i.e. two EGF molecules per s-erbB1 molecule plus two EGF molecules per one s-erbB4) increases the gradient of the straight line only slightly (circles in Figure 6), suggesting that some oligomerization is induced. Addition of only NRG1- $\beta$ 1 to the same final concentration gives a similar result (triangles in Figure 6). Since ligand is not limiting in either of these cases, we hypothesized that these small increases in gradient result from homo-oligomerization of

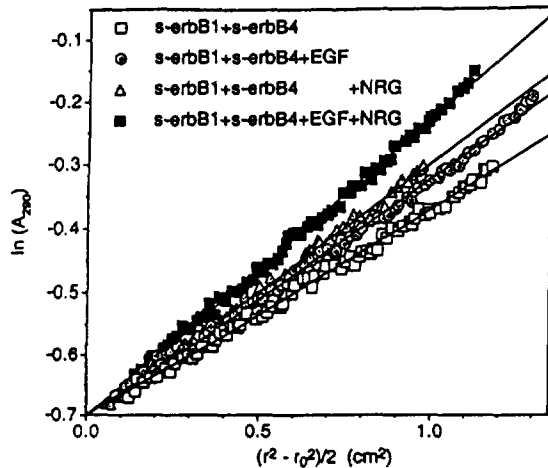


Fig. 6. Analytical ultracentrifugation data, presented as  $\ln(A_{200})$  against  $(r^2 - r_0^2)/2$  plots, to study s-erbB1-s-erbB4 hetero-oligomerization. The s-erbB1:s-erbB4 mixture (8  $\mu\text{M}$  total [s-erbB]) without ligand gives a straight line with the gradient expected for monomeric protein (open squares). Addition of EGF alone (16  $\mu\text{M}$ ) or NRG alone (16  $\mu\text{M}$ ) results in a modest increase in molecular mass that is consistent with homo-oligomerization of one species only (gray circles and triangles, respectively). Addition of both EGF and NRG (8  $\mu\text{M}$  each) results in a substantially larger increase in the gradient (black squares), indicating that both species homo-oligomerize independently, and do not form hetero-oligomers (see text for explanation).

just s-erbB1 when EGF is added, and of just s-erbB4 when NRG1- $\beta$ 1 is added. If this is true, an identical sample containing the same total ligand concentration, but as a 1:1 mixture of EGF and NRG1- $\beta$ 1 (i.e. with two EGF molecules per s-erbB1 molecule plus two NRG1- $\beta$ 1 molecules per one s-erbB4), should give a substantially steeper gradient, by inducing independent homo-oligomerization of both s-erbB1 and s-erbB4. Indeed, the steepest line in Figure 6 (filled squares) shows this to be the case, arguing that s-erbB1 and s-erbB4 do not form hetero-oligomers under these conditions—with either EGF or NRG1- $\beta$ 1.

#### Evidence for NRG1- $\beta$ 1-induced hetero-oligomerization of s-erbB4 and s-erbB2

The experiments described above show that EGF does not induce hetero-oligomerization of s-erbB1 with s-erbB2 or s-erbB4. Other experiments showed that EGF does not induce the formation of s-erbB1-s-erbB3 or s-erbB2-s-erbB3 hetero-oligomers, and that NRG1- $\beta$ 1 does not drive the interaction of s-erbB1 with s-erbB3 (not shown). Therefore, although EGF-induced s-erbB1 homodimerization is highly efficient, s-erbB1 does not participate in formation of any s-erbB hetero-oligomer. Furthermore, EGF cannot induce the formation of any s-erbB hetero-oligomer. To compare these properties of EGF with those of NRG1- $\beta$ 1, we next tested the ability of NRG1- $\beta$ 1 to induce formation of a series of s-erbB dimers (Figure 7). Using linearized sedimentation equilibrium data as a qualitative guide, Figure 7A, B and C shows that NRG1- $\beta$ 1 induces homo-oligomerization of s-erbB4 (see also Figures 3B and 4D), but not s-erbB2 or s-erbB3. The data for s-erbB4 homo-oligomerization (from Figure 7A) are superimposed upon all other graphs in Figure 7 to aid

comparison. NRG1- $\beta$ 1 addition to a s-erbB2:s-erbB3 mixture caused a slight increase in the gradient of the best straight line through the data (Figure 7D), suggesting that there may be very weak hetero-oligomerization of these proteins (although much weaker than s-erbB4 homo-oligomerization). The data obtained with a s-erbB3:s-erbB4 mixture (Figure 7E) are most consistent with NRG1- $\beta$ 1 inducing independent homo-oligomerization of s-erbB4, with no effect on s-erbB3 (as seen for NRG1- $\beta$ 1 addition to a s-erbB1/s-erbB4 mixture)—and therefore do not suggest a hetero-oligomerization event.

Figure 7F shows the most interesting of these results, and represents the only data in this study that argue for ligand-induced s-erbB hetero-oligomerization. In the absence of NRG1- $\beta$ 1, sedimentation of the s-erbB2:s-erbB4 mixture is indistinguishable from that of unliganded s-erbB4. When NRG1- $\beta$ 1 is added, sedimentation of the s-erbB2:s-erbB4 mixture is almost identical to that seen with s-erbB4 alone (at the same total s-erbB concentration). This argues that NRG1- $\beta$ 1 addition induces the same increase in average molecular mass regardless of whether all of the s-erbB molecules in the sample are s-erbB4, or half of them are s-erbB2. There are two possible explanations for this. One is that NRG1- $\beta$ 1 can induce homo-oligomerization of s-erbB2 (as well as that of s-erbB4), which Figure 7B shows to be false. The other explanation is that hetero-oligomers containing s-erbB2 plus s-erbB4 are induced by NRG1- $\beta$ 1 with an efficiency similar to s-erbB4 homo-oligomerization. Independent MALLS studies (not shown) also showed that the addition of 1.5-fold molar excess of NRG1- $\beta$ 1 induces the same increase in weight-averaged molecular mass for a 1:1 s-erbB2:s-erbB4 mixture as it does for a solution of s-erbB4 alone, again suggesting NRG1- $\beta$ 1-induced s-erbB2-s-erbB4 hetero-oligomerization.

#### Discussion

Using analytical ultracentrifugation and MALLS, we have shown that EGF induces efficient homodimerization of the EGF receptor extracellular domain (s-erbB1), but does not induce formation of any detectable hetero-oligomers (or other homo-oligomers) of erbB receptor extracellular domains. Similar studies with NRG1- $\beta$ 1 showed that this ligand induces efficient homo-oligomerization of the erbB4 extracellular domain (s-erbB4), but no other s-erbB homo-oligomers. The s-erbB4 oligomers induced by NRG1- $\beta$ 1 appear to be larger than dimers, although we have not yet established their maximum size. As well as inducing s-erbB4 homo-oligomerization, NRG1- $\beta$ 1 appears to stabilize the formation of hetero-oligomers containing both s-erbB4 and s-erbB2. The qualitative results of our studies are summarized in Table II.

#### Comparisons with previous studies

The  $K_D$  value reported in Table I for EGF binding by s-erbB1 (118 nM) is comparable with values previously reported (100–500 nM) for EGF binding by monomeric s-erbB1 (Greenfield *et al.*, 1989; Günther *et al.*, 1990; Hurwitz *et al.*, 1991; Lax *et al.*, 1991; Zhou *et al.*, 1993; Brown *et al.*, 1994; Lemmon *et al.*, 1997). However, the data in Figure 3A suggest that the s-erbB1 used here dimerizes at least 15-fold more strongly upon EGF binding

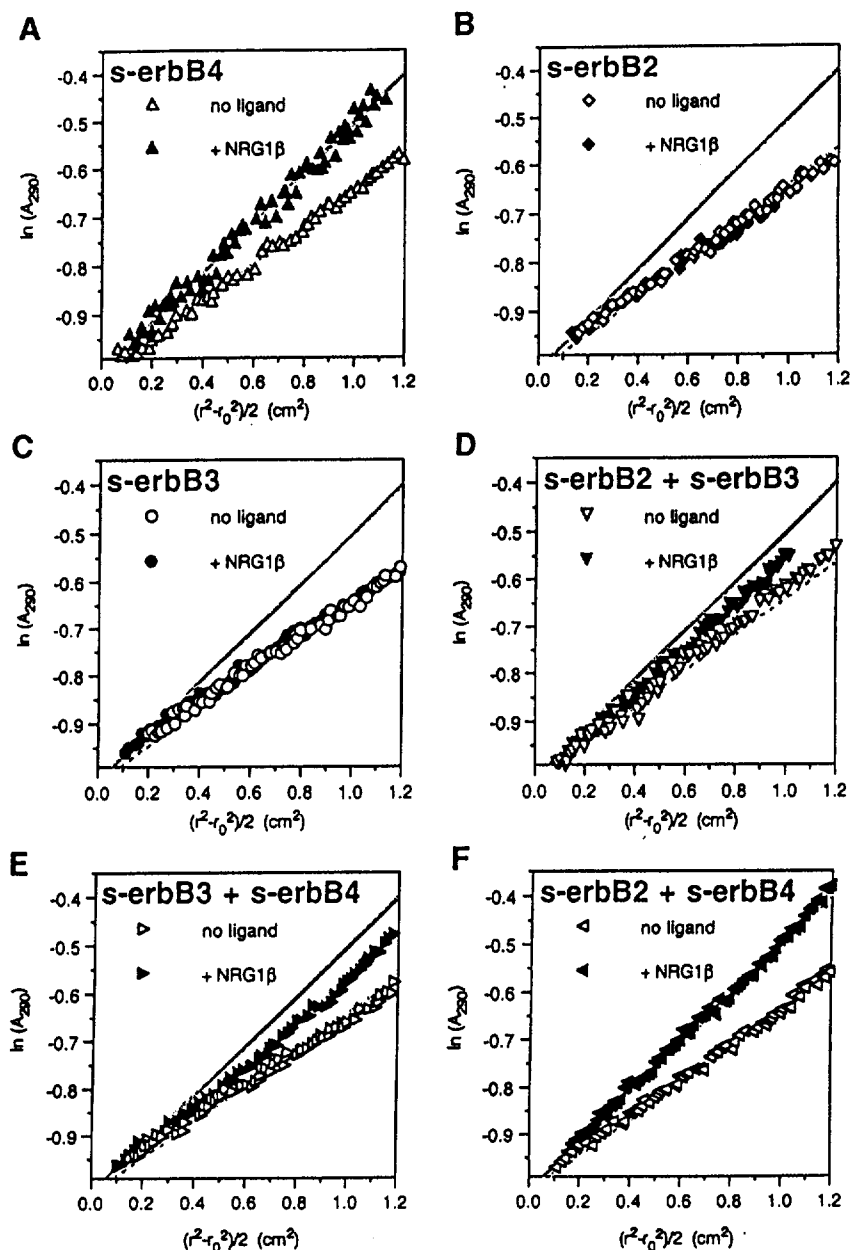


Fig. 7. Plots of  $\ln(\text{Abs})$  against  $(r^2 - r_0^2)/2$  for different pairwise mixtures of s-erbB2, s-erbB3 and s-erbB4 with (open symbols) and without (filled symbols) added NRG1- $\beta$ 1. (A) The increase in gradient of the  $\ln(\text{Abs})$  against  $(r^2 - r_0^2)/2$  plot that results from NRG1- $\beta$ 1-induced homo-oligomerization of s-erbB4. Lines corresponding to these data are superimposed in gray on each other graph in the figure. (B and C) NRG1- $\beta$ 1 fails to induce homo-oligomerization of s-erbB2 or s-erbB3. The data in (D) suggest that s-erbB2 and s-erbB3 may form very weak hetero-oligomers upon NRG1- $\beta$ 1 addition. As seen for s-erbB1 and s-erbB2 in Figure 5B, the data in (E) argue that s-erbB3 does not form hetero-oligomers with s-erbB4. The correspondence (F) of the line for the s-erbB2/s-erbB4 + NRG1- $\beta$ 1 sample with that for NRG1- $\beta$ 1-induced s-erbB4 oligomers shown in (A) indicates that NRG1- $\beta$ 1 can induce formation of s-erbB2-s-erbB4 hetero-oligomers (see text for details). Experiments were performed with a total s-erbB concentration of 10  $\mu\text{M}$ , to which was added a 2-fold molar excess of NRG1- $\beta$ 1.

than material used in our earlier studies. Whereas the  $K_D$  for dimerization of a 1:1 EGF:s-erbB1 complex was estimated previously as 3.3  $\mu\text{M}$  (Lemmon *et al.*, 1997), in which case it would be <50% dimeric in Figure 3A, the protein used in this study remained completely dimeric at concentrations as low as 250 nM (not shown). This difference may reflect the fact that, rather than using chaotropes to elute the protein from immunoaffinity columns, s-erbB1 produced for this study was purified under milder conditions, using metal affinity chromatography (see Materials and methods).

The  $K_D$  value reported for s-erbB3 binding to the EGF domain of NRG1- $\beta$ 1 (249 nM; Table I) is ~10-fold weaker than the value reported for its binding to full-length NRG1- $\beta$ 2 in analytical ultracentrifugation studies (Horan *et al.*, 1995). This difference may reflect the use of alternative NRG1- $\beta$  isoforms in the two studies or, more likely, a contribution to s-erbB3 binding by regions of full-length NRG1- $\beta$ 2 outside the EGF domain (although the EGF domain is sufficient for all known biological activities of NRG1; Holmes *et al.*, 1992). In agreement with our findings (Figures 4C and 7), Horan *et al.* (1995)

Table II. Summary of ligand-induced s-erbB oligomers observed

|         | s-erbB1 |                 | s-erbB2 |                 | s-erbB3 |                 | s-erbB4 |                 |
|---------|---------|-----------------|---------|-----------------|---------|-----------------|---------|-----------------|
|         | EGF     | NRG1- $\beta$ 1 | EGF     | NRG1- $\beta$ 1 | EGF     | NRG1- $\beta$ 1 | EGF     | NRG1- $\beta$ 1 |
| s-erbB1 | homo    | -               | -       | -               | -       | -               | -       | -               |
| s-erbB2 | -       | -               | -       | -               | -       | hetero (weak)   | -       | hetero          |
| s-erbB3 | -       | -               | -       | -               | -       | -               | -       | -               |
| s-erbB4 | -       | -               | -       | -               | -       | -               | -       | homo            |

did not detect s-erbB3 homodimerization or s-erbB2-s-erbB3 heterodimerization upon NRG1- $\beta$ 2 binding.

#### Implications for erbB receptor oligomerization

As stated in the Introduction, we set out to test the hypothesis that the mechanism of erbB receptor transmodulation involves simple formation of receptor heterodimers upon binding to one or another bivalent ligand (Alroy and Yarden, 1997; Lemmon *et al.*, 1997; Tzahar *et al.*, 1997). We found that, in common with almost every other RTK extracellular domain that has been studied (Lemmon and Schlessinger, 1994; Heldin, 1995), the erbB1 and erbB4 extracellular domains form homo-oligomers upon binding to their respective ligands (EGF and NRG1- $\beta$ 1). As with other well-characterized examples, this homo-oligomerization may be driven by bivalent erbB ligand binding. However, we could only detect the formation of one of the six possible pairwise s-erbB hetero-oligomers; s-erbB4 forming co-oligomers with s-erbB2 upon NRG1- $\beta$ 1 binding. EGF did not induce any s-erbB oligomer other than s-erbB1 homodimers, and our data suggest that the one hetero-oligomer that we could detect (s-erbB2-s-erbB4) is likely to be larger than a dimer.

These observations suggest that the simple erbB receptor heterodimerization hypothesis, in which ligand binding drives the heteromeric association of two different erbB receptors through their extracellular ligand-binding domains, is false. Instead, our findings argue that the mechanisms of ligand-induced erbB receptor homo- and hetero-oligomerization must be fundamentally different. In particular, the fact that ligand-induced erbB1 and erbB4 homo-oligomerization can be recapitulated with the isolated extracellular domains of these receptors, while hetero-oligomerization cannot, suggests that regions outside the extracellular domain are required for heteromeric, but not homomeric, interactions of the intact forms of these receptors.

#### A model for 'homodimer-nucleated' erbB receptor transmodulation

There are  $\sim 10^4$ - $10^5$  erbB1 or erbB4 receptors on the surface of a typical EGF- or NRG-responsive cell. For a cell with a radius of 8  $\mu$ m, this receptor density translates to an effective local concentration of 0.1-3  $\mu$ M at the very least. More reasonable estimates that account for orientation effects would be 10-100 times higher (Grasberger *et al.*, 1986). All experiments presented herein were performed with s-erbB proteins at concentrations of 4-10  $\mu$ M, mimicking the effective erbB receptor concentra-

tion at the cell surface. Since liganded s-erbB1 and s-erbB4 homo-oligomerize so strongly under these conditions, we suggest that homo-oligomerization of the intact membrane-anchored receptors is likely to be the first response to ligand binding *in vivo*. It seems unlikely that ligand-induced hetero-oligomerization events that we cannot detect in the studies described here (driven by regions outside the extracellular domains) would compete with these strong, directly ligand-induced, homomeric interactions. We therefore suggest that the ligand-induced erbB receptor hetero-oligomers seen in many studies of intact erbB receptors are 'nucleated' by ligand-induced erbB1 or erbB4 homo-oligomers, and most probably represent something larger than a heterodimer. Huang *et al.* (1998) have suggested a similar model, as outlined in the Introduction, in which a ligand-induced homodimer of one receptor (e.g. erbB1) transactivates a second receptor (e.g. erbB2) by inducing its dimerization. In the resulting heterotetramer, the two molecules of the second (unliganded) receptor could activate one another through trans-autophosphorylation, and may be identical or different (if different, the 'secondary dimerization' observations made by Gamett *et al.*, 1997 could be explained). A 'homodimer-nucleated' hetero-tetramer model of this sort could explain the initially surprising finding that a kinase-negative mutant of erbB1 is nonetheless able to mediate EGF-induced transmodulation of erbB2 (Wright *et al.*, 1995). According to the model, an EGF-induced homodimer of the erbB1 mutant would transactivate erbB2 by inducing erbB2 homodimerization (and consequent activation) within the context of a heterotetramer—the kinase activity of erbB1 would not be required. The model could also explain how an erbB2 mutant with its intracellular domain deleted can inhibit transmodulation of endogenous erbB2 in a dominant-negative manner (Jones and Stern, 1999).

While this homodimer-nucleated heterotetramer model may explain transmodulation mediated by erbB1 or erbB2, it cannot readily explain the formation of erbB2-erbB3 hetero-oligomers. We and others (Horan *et al.*, 1995; Tzahar *et al.*, 1997) have failed to detect NRG-induced homodimerization of the erbB3 extracellular domain using biophysical or cross-linking methods. However, NRG-induced homo-oligomerization of intact (or truncated) erbB3 in cells has been detected in chemical cross-linking studies (Sliwkowski *et al.*, 1994; Tzahar *et al.*, 1997). Unlike erbB1 or erbB4, erbB3 appears to require more than just the extracellular domain for its ligand-induced homo-oligomerization. Tzahar *et al.* (1997) have presented evidence suggesting that transmembrane domain

interactions may be important for both homo- and hetero-oligomeric interactions of erbB3. An NRG-induced erbB3 oligomer, stabilized by such interactions, could transmodulate erbB2 by inducing its 'proxy' dimerization in the model discussed above (see also Huang *et al.*, 1998).

### Relationship of hetero-oligomer formation to ligand binding

Despite the fact that it does not bind either ligand independently, overexpression of erbB2 increases the NRG-binding affinity of cells that express erbB3 (Sliwkowski *et al.*, 1994; Karunakaran *et al.*, 1996) and the EGF-binding affinity of cells that express erbB1 (Karunakaran *et al.*, 1996). In an effort to understand these effects, Sliwkowski and colleagues investigated how forced heterodimerization of erbB receptor extracellular domains alters their ligand-binding properties. Hetero- (and homo-) dimerization was forced by fusing erbB receptor extracellular domains to the (dimeric) hinge and  $F_c$  portions of IgG<sub>1</sub> heavy chain. Heterodimeric IgG fusions containing the erbB2 extracellular domain alongside that of erbB3 or erbB4 bound NRG1- $\beta$  significantly more strongly than erbB3 or erbB4 homodimer fusion (Fitzpatrick *et al.*, 1998; J.T.Jones *et al.*, 1999). In contrast, a heterodimer containing the extracellular domains of erbB2 and erbB1 was indistinguishable from the equivalent erbB1 homodimer in its binding to EGF, TGF- $\alpha$ , HB-EGF or betacellulin (J.T.Jones *et al.*, 1999). This difference suggests that erbB2 enhances NRG and EGF binding through distinct mechanisms. While NRG binding may be enhanced simply by receptor extracellular domain heteromerization, some other mechanism must be invoked for the enhancement of cellular EGF binding by overexpression of erbB2 (Karunakaran *et al.*, 1996). Our studies of s-erbB oligomerization suggest a similar distinction: while the isolated extracellular domains cannot recapitulate ligand-induced erbB1-erbB2 hetero-oligomerization, at least NRG-induced erbB2-erbB4 heteromerization could be reproduced with the soluble s-erbB proteins studied here.

### Conclusions

Regardless of the precise mechanism of ligand-induced erbB receptor hetero-oligomerization, the results presented here show that isolated extracellular domains reproduce ligand-induced homomeric interactions of erbB receptors more faithfully than their reported heteromeric interactions. This finding alone argues that the mechanisms for homo- and hetero-oligomerization of the erbB receptors must differ. Our data therefore provide strong evidence against the simple heterodimerization hypothesis that we set out to test. Rather, in agreement with suggestions made by other groups (Gamett *et al.*, 1997; Huang *et al.*, 1998), we suggest that the ligand-induced erbB homo-oligomers that can be formed with isolated extracellular domains nucleate larger erbB hetero-oligomers through interactions that may also involve other regions of the receptor. Transphosphorylation within these larger 'homodimer-nucleated' hetero-oligomers may be responsible for erbB receptor transmodulation.

## Materials and methods

### Generation of s-erbB constructs

A fragment of human erbB1 cDNA directing expression of residues 1-642 (1-618 of the mature sequence), followed by a hexahistidine tag and stop codon, was subcloned into pFastBac1 (Life Technologies Inc). The 1955 bp fragment was generated by PCR, introducing a unique *Bgl*II site immediately before the initiation codon and a unique *Xba*I site that follows the introduced stop codon. The 1955 bp *Bgl*II-*Xba*I-digested PCR product was ligated into *Bam*HI-*Xba*I-digested pFastBac1. To minimize the risk of PCR artifacts, a 1260 bp *Eco*RI-*Apa*I fragment of this PCR-derived clone was swapped for the equivalent region from the original erbB1 cDNA. A fragment of human erbB2 cDNA, directing expression of residues 1-647 (1-628 of the mature sequence), was generated similarly. In this case, a unique *Xba*I site was introduced before the initiation codon, and a unique *Hind*III site was introduced after the histidine tag and stop codon. The 1980 bp *Xba*I-*Hind*III-digested PCR product was ligated into *Xba*I-*Hind*III-digested pFastBac1. An 1880 bp internal fragment of this PCR product, extending from an *Nco*I site at the initiation codon to a unique *Sph*I site, was then swapped for the equivalent fragment from the original erbB2 cDNA.

Fragments encoding human erbB3 residues 1-639 (1-620 of the mature protein) and human erbB4 residues 1-649 (1-624 of the mature protein), with a unique *Bam*HI site at one end and an *Xba*I site at the other, were generated by PCR, and ligated into *Bam*HI-*Xba*I-digested pFastBac1. The sequence of all PCR-derived fragments and their cloning boundaries were confirmed by automated dideoxynucleotide sequencing methods.

### Protein production

Typically, 5-10 l of Sf9 cells were grown as a suspension culture in Sf900-II medium (Gibco-BRL) using multiple 1 l spinner flasks that each contained <500 ml of medium (to ensure adequate aeration). At a cell density of  $2.5 \times 10^6$  cells/ml (viability >98%), freshly amplified high-titer virus stock was added to a multiplicity of infection (m.o.i.) of ~5. Cultures were incubated at 27°C for a further 96 h. Clarified conditioned medium was concentrated 2-fold, and then diafiltered against 3.5 vols of 25 mM Tris-HCl, 150 mM NaCl, pH 8.0 (buffer A), using a Millipore Prep/Scale-TFF 30 kDa cartridge. The solution was concentrated further to ~300 ml prior to loading onto a 5 ml Ni-NTA Superflow column (Qiagen). After extensive washing with buffer A, the column was washed sequentially with two column volumes of buffer A containing 30, 50, 75, 100 and 300 mM imidazole, pH 8.0. Typically, most s-erbB protein eluted in the 75 and 100 mM fractions. Fractions were concentrated in a Centrprep 30 (Amicon), and loaded onto a Pharmacia Superose 6 gel filtration column in 25 mM HEPES, pH 8.0, 100 mM NaCl, from which they eluted as ~85 kDa species. For s-erbB1 and s-erbB4, appropriate gel filtration fractions were pooled, diluted 1.5-fold with 50 mM MES pH 6.0, and were loaded on to an BioScale-S2 cation exchange column (BioRad) pre-equilibrated with 25 mM MES pH 6.0. Protein was eluted with a gradient in NaCl, s-erbB1 eluting at ~200 mM NaCl and s-erbB4 at ~300 mM NaCl. Attempts to purify s-erbB2 and s-erbB3 by ion exchange led to precipitation of the proteins at the low salt concentration required for column binding. Purified s-erbB proteins were buffer exchanged into 25 mM HEPES, 100 mM NaCl, pH 8.0, concentrated to between 20 and 100  $\mu$ M, and stored at 4°C. Purity was checked by SDS-PAGE (Figure 1), and concentrations were determined by absorbance at 280 nm using extinction coefficients calculated as described (Mach *et al.*, 1992) of 56 920/M/cm (s-erbB1), 62 460/M/cm (s-erbB2), 63 940/M/cm (s-erbB3) and 74 300/M/cm (s-erbB4). We previously had used quantitative amino acid analysis to measure a value of 58 500/M/cm for s-erbB1 from mammalian cells (Lemmon *et al.*, 1997); this value is within 3% of that calculated according to Mach *et al.* (1992). Calculated extinction coefficients of 18 780/M/cm (EGF) and 5920/M/cm (NRG1- $\beta$ 1) were also used for determination of ligand concentration.

Approximate final yields of purified protein from 1 l of conditioned medium were 1 (s-erbB1), 0.2 (s-erbB2), 1 (s-erbB3) and 0.5 mg (s-erbB4). Ligands used for this study were purchased from Interger (human EGF) or R & D Systems (human NRG1- $\beta$ 1).

### Multi-angle laser light-scattering (MALLS) studies

A DAWN DSP laser photometer from Wyatt Technologies (Santa Barbara, CA) was used for MALLS studies (Wyatt, 1993). The instrument was used in micro-batch mode, with samples being introduced into the flow cell via a 0.1  $\mu$ m filter using a syringe pump. To avoid introduction of air bubbles, concentrated protein solutions were diluted to

working concentrations in degassed buffer, and samples were introduced into the flow cell via a low dead volume multi-port valve that was loaded with several samples and purged of air prior to a series of measurements. Scattering data at all 17 angles were collected until maximum stable scattering for a sample was seen, which can be achieved at flow rates of 2 ml/h with samples of ~300  $\mu$ l. Scattering data were collected and analyzed using ASTRA software (Wyatt Technologies) supplied with the instrument. Relative weight-averaged molecular masses were determined from the scattering data collected for a given ligand:receptor mixture (once stabilized) using Debye plots, in which  $R(\theta)/K^*$  is plotted against  $\sin^2(\theta/2)$ , where  $\theta$  is the scattering angle;  $R(\theta)$  is the excess intensity ( $I$ ) of scattered light at that angle;  $c$  is the concentration of the sample; and  $K^*$  is a constant equal to  $4\pi^2 n^2 (dn/dc)^2 / \lambda_0^4 N_A$  (where  $n$  = solvent refractive index,  $dn/dc$  = refractive index increment of scattering sample,  $\lambda_0$  = wavelength of scattered light and  $N_A$  = Avogadro's number). Extrapolation of a Debye plot to zero angle gives an estimate of the weight-averaged molecular mass ( $\bar{M}_w$ ) (Wyatt, 1993).  $\bar{M}_w$  is defined as:

$$\bar{M}_w = \frac{\sum_i n_i M_i^2}{\sum_i n_i M_i}$$

for  $n$  moles of  $i$  different species with molecular weight  $M_i$ .

In ligand titration experiments, the contribution of added ligand to the mass concentration was neglected (see also Lemmon *et al.*, 1997). Since we are interested in dimerization, i.e. only the 'fold increase' in  $\bar{M}_w$ , our results are not affected by the value of  $K^*$ , of which we are uncertain since we have not determined the extent of glycosylation of the s-erbB proteins accurately. MALLS data are therefore discussed in terms of 'fold increase' in  $\bar{M}_w$  over that measured for s-erbB protein alone. Where estimates for  $\bar{M}_w$  are reported, mass concentrations were converted from molar concentrations using the molecular weight suggested by the amino acid sequence, and assuming that s-erbB glycoproteins are 20% carbohydrate by mass.

#### Analytical ultracentrifugation studies

Sedimentation equilibrium experiments employed the XL-A analytical ultracentrifuge (Beckman). Samples were loaded into six-channel epon charcoal-filled centerpiece, using quartz windows. Experiments were performed at 20°C, detecting at 280–300 nm, using three different speeds (6000, 9000 and 12 000 r.p.m.), with very similar results. Solvent density was taken as 1.003 g/ml, and the partial specific volumes of the s-erbB proteins were approximated from their amino acid compositions and the assumption of ~20% carbohydrate as 0.71 ml/g for the purposes described here. Experiments were performed at 5–10  $\mu$ M protein. Data were fit using the Optima XL-A data analysis software (Beckman/MicroCal) to models assuming a single non-ideal species for unliganded s-erbB proteins. When ligand was added, a two-species fit was used, in which one of the species was the excess ligand (partial specific volume 0.74 ml/g), which sediments as a 6 kDa (EGF) or 8 kDa (NRG) species (not shown). The molecular mass of the ligand species was fixed in these fits, while the mass and concentration of the receptor species were allowed to float. Goodness of fit was judged by the occurrence of randomly distributed residuals, examples of which are shown in Figure 4. For more complicated mixtures of receptors and ligands, simple qualitative interpretations of analytical ultracentrifugation experiments were made by inspection when possible (see Figures 5B, 6 and 7).

#### BIAcore studies

BIAcore binding experiments employed a BIAcore 2000 instrument, and were performed in 10 mM HEPES buffer, pH 7.4, that contained 150 mM NaCl, 3.4 mM EDTA and 0.005% Tween-20 at 25°C. The hydrogel matrix of BIAcore CM5 Biosensor chips was activated with *N*-hydroxysuccinimide (NHS) and *N*-ethyl-*N'*-(3-(diethylamino)propyl) carbodiimide (EDC). EGF (at 200  $\mu$ g/ml) in 10 mM sodium acetate, pH 4.0, or NRG1- $\beta$ 1 (at 200  $\mu$ g/ml) in 10 mM sodium acetate, pH 4.8, was then flowed over the activated surface at 5  $\mu$ l/min for 10 min. Non-cross-linked ligand was removed, and unreacted sites were blocked with 1 M methanolamine, pH 8.5. The signal contributed by immobilized EGF or NRG1- $\beta$ 1 ranged from 150 to 400 RU, depending on the specific chip.

Purified s-erbB proteins at a series of concentrations were each flowed simultaneously over the EGF and NRG1- $\beta$ 1 (and mock/control) surfaces at 5  $\mu$ l/min for 7 min, by which time binding had reached a plateau in each case. The RU value corresponding to this plateau was taken as a measure of s-erbB protein binding, and was corrected for background non-specific

binding and bulk refractive index effects by subtraction of data obtained in parallel using the mock-coupled hydrogel surface. RU values were then converted into percentage maximal binding. This conversion was performed separately for each surface (since levels of immobilization varied); 100% binding was defined for an NRG surface as the highest corrected signal seen with s-erbB3 and s-erbB4 (which were always the same to within 10%), and for an EGF surface the highest corrected signal seen with s-erbB1. Buffer washes between runs were sufficient to bring the RU value back down to baseline. Data were plotted as s-erbB concentration against percentage maximal binding, and fit to a simple binding equation in ORIGIN (MicroCal) to estimate the  $K_D$ .

#### Acknowledgements

We thank Irit Lax, Yossi Schlessinger, Greg Van Duynne and members of the Lemmon laboratory for many valuable discussions and comments on the manuscript. BIAcore experiments were performed in the Biosensor Interaction Analysis Core at Penn. This work was supported by grants from the National Institutes of Health (CA79992 to M.A.L.), the US Army Breast Cancer Research Program (DAMD17-98-1-8232 to M.A.L., and DAMD17-98-1-8228 to K.M.F.), a Scholar Award from the Cancer Research Fund of the Damon Runyon-Walter Winchell Foundation (to M.A.L.) and the Research Foundation of the University of Pennsylvania.

#### References

- Alroy, I. and Yarden, Y. (1997) The ErbB signaling network in embryogenesis and oncogenesis: signal diversification through combinatorial ligand-receptor interactions. *FEBS Lett.*, **410**, 83–86.
- Brown, P.M., Debanne, M.T., Grothe, S., Bergsma, D., Caron, M., Kay, C. and O'Connor-McCourt, M.D. (1994) The extracellular domain of the epidermal growth factor receptor. Studies on the affinity and stoichiometry of binding, receptor dimerization and a binding-domain mutant. *Eur. J. Biochem.*, **225**, 223–233.
- Burden, S. and Yarden, Y. (1997) Neuregulins and their receptors: a versatile signaling module in organogenesis and oncogenesis. *Neuron*, **18**, 847–855.
- Cantor, C.R. and Schimmel, P.R. (1980) *Biophysical Chemistry: Techniques for the Study of Biological Structure and Function*. W.H. Freeman and Co., New York.
- Carraway, K.L., III and Cantley, L.C. (1994) A Neu acquaintance for erbB3 and erbB4: a role for receptor heterodimerization in growth signaling. *Cell*, **78**, 5–8.
- Cohen, B.D., Green, J.M., Foy, L. and Fell, H.P. (1996) HER4-mediated biological and biochemical properties in NIH 3T3 cells. Evidence for HER1-HER4 heterodimers. *J. Biol. Chem.*, **271**, 4813–4818.
- Fitzpatrick, V.D., Pisacane, P.I., Vandlen, R.L. and Sliwkowski, M.X. (1998) Formation of a high-affinity heregulin binding site using the soluble extracellular domains of ErbB2 with ErbB3 or ErbB4. *FEBS Lett.*, **431**, 102–106.
- Gamett, D.C., Pearson, G., Cerione, R.A. and Friedberg, I. (1997) Secondary dimerization between members of the epidermal growth factor receptor family. *J. Biol. Chem.*, **272**, 12052–12056.
- Goldman, R., Levy, R.B., Peles, E. and Yarden, Y. (1990) Heterodimerization of the erbB-1 and erbB-2 receptors in human breast carcinoma cells: a mechanism for receptor transregulation. *Biochemistry*, **29**, 11024–11028.
- Grasberger, B., Minton, A.P., DeLisi, C. and Metzger, H. (1986) Interaction between proteins localized in membranes. *Proc. Natl. Acad. Sci. USA*, **83**, 6258–6262.
- Graus-Porta, D., Beerli, R.R., Daly, J.M. and Hynes, N.E. (1997) ErbB-2, the preferred heterodimerization partner of all ErbB receptors, is a mediator of lateral signaling. *EMBO J.*, **16**, 1647–1655.
- Greenfield, C., Hiles, I., Waterfield, M.D., Federwisch, M., Wollmer, A., Blundell, T.L. and McDonald, N. (1989) Epidermal growth factor binding induces a conformational change in the external domain of its receptor. *EMBO J.*, **8**, 4115–4123.
- Günther, N., Betzel, C. and Weber, W. (1990) The secreted form of the epidermal growth factor receptor: characterization and crystallization of the receptor-ligand complex. *J. Biol. Chem.*, **265**, 22082–22085.
- Harari, D., Tzahar, E., Romano, J., Shelly, M., Pierce, J.H., Andrews, G.C. and Yarden, Y. (1999) Neuregulin-4: a novel growth factor that acts through the ErbB-4 receptor tyrosine kinase. *Oncogene*, **18**, 2681–2689.

- Heldin, C.-H. (1995) Dimerization of cell surface receptors in signal transduction. *Cell*, 80, 213-223.
- Holmes, W.E. *et al.* (1992) Identification of heregulin, a specific activator of p185<sup>erbB2</sup>. *Science*, 256, 1205-1210.
- Honegger, A.M., Schmidt, A., Ullrich, A. and Schlessinger, J. (1990) Evidence for epidermal growth factor (EGF)-induced intermolecular autophosphorylation in living cells. *Mol. Cell. Biol.*, 10, 4035-4044.
- Horan, T., Wen, J., Arakawa, T., Liu, N., Brankow, D., Hu, S., Ratzkin, B. and Philo, J.S. (1995) Binding of Neu differentiation factor with the extracellular domain of Her2 and Her3. *J. Biol. Chem.*, 270, 24604-24608.
- Huang, G.C., Ouyang, X. and Epstein, R.J. (1998) Proxy activation of protein erbB2 by heterologous ligands implies a heterotetrameric mode of receptor tyrosine kinase interaction. *Biochem. J.*, 331, 113-119.
- Hubbard, S.R., Mohammadi, M. and Schlessinger, J. (1998) Autoregulatory mechanisms in protein-tyrosine kinases. *J. Biol. Chem.*, 273, 11987-11990.
- Hurwitz, D.R., Emanuel, S.L., Nathan, M.H., Sarver, N., Ullrich, A., Felder, S., Lax, I. and Schlessinger, J. (1991) EGF induces increased ligand binding affinity and dimerization of soluble epidermal growth factor (EGF) receptor extracellular domain. *J. Biol. Chem.*, 266, 22035-22043.
- Jones, F.E. and Stern, D.F. (1999) Expression of dominant-negative ErbB2 in the mammary gland of transgenic mice reveals a role in lobuloalveolar development and lactation. *Oncogene*, 18, 3481-3490.
- Jones, F.E., Welte, T., Fu, X.Y. and Stern, D.F. (1999) ErbB4 signaling in the mammary gland is required for lobuloalveolar development and Stat5 activation during lactation. *J. Cell Biol.*, 147, 77-88.
- Jones, J.T., Akita, R.W. and Sliwkowski, M.X. (1999) Binding specificities of egf domains for ErbB receptors. *FEBS Lett.*, 447, 227-231.
- Karunakaran, D., Tzahar, E., Beerli, R.R., Chen, X., Graus-Porta, D., Ratzkin, B.J., Seger, R., Hynes, N.E. and Yarden, Y. (1996) ErbB-2 is a common auxiliary subunit of NDF and EGF receptors: implications for breast cancer. *EMBO J.*, 15, 254-264.
- King, C.R., Borrello, I., Bellot, F., Comoglio, P. and Schlessinger, J. (1988) EGF binding to its receptor triggers a rapid tyrosine phosphorylation of the erbB2 protein in the mammary tumor cell line SKBR-3. *EMBO J.*, 7, 1647-1651.
- Lax, I., Mitra, A.K., Ravera, C., Hurwitz, D.R., Rubinstein, M., Ullrich, A., Stroud, R.M. and Schlessinger, J. (1991) Epidermal growth factor (EGF) induces oligomerization of soluble, extracellular, ligand-binding domain of EGF receptor. *J. Biol. Chem.*, 266, 13828-13833.
- Lemmon, M.A. and Schlessinger, J. (1994) Regulation of signal transduction and signal diversity by receptor oligomerization. *Trends Biochem. Sci.*, 19, 459-463.
- Lemmon, M.A., Bu, Z., Ladbury, J.E., Zhou, M., Pinchasi, D., Lax, I., Engelman, D.M. and Schlessinger, J. (1997) Two EGF molecules contribute additively to stabilization of the EGFR dimer. *EMBO J.*, 16, 281-294.
- Mach, H., Middaugh, C.R. and Lewis, R.V. (1992) Statistical determination of the average values of the extinction coefficient of tryptophan and tyrosine in native proteins. *Anal. Biochem.*, 200, 74-80.
- Qian, X., LeVe, C.M., Freeman, J.K., Dougall, W.C. and Greene, M.I. (1994) Heterodimerization of epidermal growth factor receptor and wild-type or kinase-deficient Neu: a mechanism of interreceptor kinase activation and transphosphorylation. *Proc. Natl Acad. Sci. USA*, 91, 1500-1504.
- Riese, D.J., II and Stern, D.F. (1998) Specificity within the EGF family/ ErbB receptor family signaling network. *BioEssays*, 20, 41-48.
- Riese, D.J., II, van Raaij, T.M., Plowman, G.D., Andrews, G.C. and Stern, D.F. (1995) The cellular response to neuregulins is governed by complex interactions of the erbB receptor family. *Mol. Cell. Biol.*, 15, 5770-5776.
- Riese, D.J., II, Kim, E.D., Elenius, K., Buckley, S., Klagsbrun, M., Plowman, G.D. and Stern, D.F. (1996) The epidermal growth factor receptor couples transforming growth factor- $\alpha$ , heparin-binding epidermal growth factor-like factor and amphiregulin to Neu, ErbB-3 and ErbB-4. *J. Biol. Chem.*, 271, 20047-20052.
- Schechter, Y., Hernaiz, L., Schlessinger, J. and Cuatrecasas, P. (1979) Local aggregation of hormone-receptor complexes is required for activation by epidermal growth factor. *Nature*, 278, 835-838.
- Schlessinger, J. (1979) Receptor aggregation as a mechanism for transmembrane signaling: Models for hormone action. In De Lisi, C. and Blumenthal, R. (eds), *Physical Chemistry of Cell Surface Events in Cellular Regulation*. Elsevier, pp. 89-118.
- Schlessinger, J. (1994) SH2/SH3 signaling proteins. *Curr. Opin. Genet. Dev.*, 4, 25-30.
- Schlessinger, J. and Ullrich, A. (1992) Growth factor signaling by receptor tyrosine kinases. *Neuron*, 9, 383-391.
- Sliwkowski, M.X. *et al.* (1994) Coexpression of erbB2 and erbB3 proteins reconstitutes a high affinity receptor for heregulin. *J. Biol. Chem.*, 269, 14661-14665.
- Sliwkowski, M.X., Lofgren, J.A., Lewis, G.D., Hotaling, T.E., Fendly, B.M. and Fox, J.A. (1999) Nonclinical studies addressing the mechanism of action of trastuzumab (Herceptin). *Semin. Oncol.*, 26 (Suppl. 12), 60-70.
- Songyang, Z. *et al.* (1993) SH2 domains recognize specific phosphopeptide sequences. *Cell*, 72, 767-778.
- Spivak-Kroizman, T., Rotin, D., Pinchasi, D., Ullrich, A., Schlessinger, J. and Lax, I. (1992) Heterodimerization of c-erbB2 with different epidermal growth factor receptor mutants elicits stimulatory or inhibitory responses. *J. Biol. Chem.*, 267, 8056-8063.
- Stern, D.F. and Kamps, M.P. (1988) EGF-stimulated tyrosine phosphorylation of p185<sup>neu</sup>: a potential model for receptor interactions. *EMBO J.*, 7, 995-1001.
- Tzahar, E. *et al.* (1997) Bivalence of EGF-like ligands drives the ErbB signaling network. *EMBO J.*, 16, 4938-4950.
- Wada, T., Qian, X. and Greene, M.I. (1990) Intermolecular association of the p185<sup>neu</sup> protein and EGF modulates EGF receptor function. *Cell*, 61, 1339-1347.
- Wright, J.D., Reuter, C.W.M. and Weber, M.J. (1995) An incomplete program of cellular tyrosine phosphorylations induced by kinase-defective epidermal growth factor receptors. *J. Biol. Chem.*, 270, 12085-12093.
- Wyatt, P.J. (1993) Light scattering and the absolute characterization of macromolecules. *Anal. Chim. Acta*, 272, 1-40.
- Yarden, Y. and Schlessinger, J. (1987a) Self-phosphorylation of epidermal growth factor receptor: evidence for a model of intermolecular allosteric activation. *Biochemistry*, 26, 1434-1442.
- Yarden, Y. and Schlessinger, J. (1987b) Epidermal growth factor induces rapid, reversible aggregation of the purified epidermal growth factor receptor. *Biochemistry*, 26, 1443-1451.
- Zhang, K., Sun, J., Liu, N., Wen, D., Chang, D., Thomason, A. and Yoshinaga, S.K. (1996) Transformation of NIH3T3 cells by HER3 or HER4 receptors requires the presence of HER1 or HER2. *J. Biol. Chem.*, 271, 3884-3890.
- Zhou, M., Felder, S., Rubinstein, M., Hurwitz, D.R., Ullrich, A., Lax, I. and Schlessinger, J. (1993) Real-time measurements of kinetics of EGF binding to soluble EGF receptor monomers and dimers support the dimerization model for receptor activation. *Biochemistry*, 32, 8193-8198.

Received June 7, 2000; accepted July 11, 2000



## NOTICE

USING GOVERNMENT DRAWINGS, SPECIFICATIONS, OR OTHER DATA INCLUDED IN THIS DOCUMENT FOR ANY PURPOSE OTHER THAN GOVERNMENT PROCUREMENT DOES NOT IN ANY WAY OBLIGATE THE U.S. GOVERNMENT. THE FACT THAT THE GOVERNMENT FORMULATED OR SUPPLIED THE DRAWINGS, SPECIFICATIONS, OR OTHER DATA DOES NOT LICENSE THE HOLDER OR ANY OTHER PERSON OR CORPORATION; OR CONVEY ANY RIGHTS OR PERMISSION TO MANUFACTURE, USE, OR SELL ANY PATENTED INVENTION THAT MAY RELATE TO THEM.

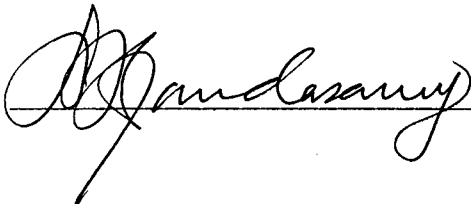
### LIMITED RIGHTS LEGEND

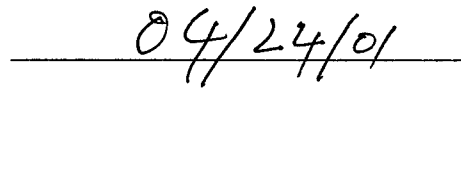
Award Number: DAMD17-98-1-8228

Organization: University of Pennsylvania

Those portions of the technical data contained in this report marked as limited rights data shall not, without the written permission of the above contractor, be (a) released or disclosed outside the government, (b) used by the Government for manufacture or, in the case of computer software documentation, for preparing the same or similar computer software, or (c) used by a party other than the Government, except that the Government may release or disclose technical data to persons outside the Government, or permit the use of technical data by such persons, if (i) such release, disclosure, or use is necessary for emergency repair or overhaul or (ii) is a release or disclosure of technical data (other than detailed manufacturing or process data) to, or use of such data by, a foreign government that is in the interest of the Government and is required for evaluational or informational purposes, provided in either case that such release, disclosure or use is made subject to a prohibition that the person to whom the data is released or disclosed may not further use, release or disclose such data, and the contractor or subcontractor or subcontractor asserting the restriction is notified of such release, disclosure or use. This legend, together with the indications of the portions of this data which are subject to such limitations, shall be included on any reproduction hereof which includes any part of the portions subject to such limitations.

THIS TECHNICAL REPORT HAS BEEN REVIEWED AND IS APPROVED FOR PUBLICATION.

  
\_\_\_\_\_

  
\_\_\_\_\_



DEPARTMENT OF THE ARMY  
US ARMY MEDICAL RESEARCH AND MATERIEL COMMAND  
504 SCOTT STREET  
FORT DETRICK, MARYLAND 21702-5012

REPLY TO  
ATTENTION OF:

MCMR-RMI-S (70-1y)

26 Aug 02

MEMORANDUM FOR Administrator, Defense Technical Information  
Center (DTIC-OCA), 8725 John J. Kingman Road, Fort Belvoir,  
VA 22060-6218


SUBJECT: Request Change in Distribution Statement

1. The U.S. Army Medical Research and Materiel Command has reexamined the need for the limitation assigned to technical reports written for this Command. Request the limited distribution statement for the enclosed accession numbers be changed to "Approved for public release; distribution unlimited." These reports should be released to the National Technical Information Service.

2. Point of contact for this request is Ms. Kristin Morrow at DSN 343-7327 or by e-mail at Kristin.Morrow@det.amedd.army.mil.

FOR THE COMMANDER:

Encl

  
PHYLLIS M. RINEHART  
Deputy Chief of Staff for  
Information Management

|           |           |
|-----------|-----------|
| ADB274369 | ADB274596 |
| ADB256383 | ADB258952 |
| ADB264003 | ADB265976 |
| ADB274462 | ADB274350 |
| ADB266221 | ADB274346 |
| ADB274470 | ADB257408 |
| ADB266221 | ADB274474 |
| ADB274464 | ADB260285 |
| ADB259044 | ADB274568 |
| ADB258808 | ADB266076 |
| ADB266026 | ADB274441 |
| ADB274658 | ADB253499 |
| ADB258831 | ADB274406 |
| ADB266077 | ADB262090 |
| ADB274348 | ADB261103 |
| ADB274273 | ADB274372 |
| ADB258193 |           |
| ADB274516 |           |
| ADB259018 |           |
| ADB231912 |           |
| ADB244626 |           |
| ADB256677 |           |
| ADB229447 |           |
| ADB240218 |           |
| ADB258619 |           |
| ADB259398 |           |
| ADB275140 |           |
| ADB240473 |           |
| ADB254579 |           |
| ADB277040 |           |
| ADB249647 |           |
| ADB275184 |           |
| ADB259035 |           |
| ADB244774 |           |
| ADB258195 |           |
| ADB244675 |           |
| ADB257208 |           |
| ADB267108 |           |
| ADB244889 |           |
| ADB257384 |           |
| ADB270660 |           |
| ADB274493 |           |
| ADB261527 |           |
| ADB274286 |           |
| ADB274269 |           |
| ADB274592 |           |
| ADB274604 |           |